

## Next generation electric drives for HEV/EV propulsion systems: Technology, trends and challenges



I. López<sup>a,\*</sup>, E. Ibarra<sup>b</sup>, A. Matallana<sup>b</sup>, J. Andreu<sup>b</sup>, I. Kortabarria<sup>b</sup>

<sup>a</sup> Department of Electrical Engineering, UPV/EHU, Plaza Ing. Torres Quevedo 1, 48013, Bilbao, Spain

<sup>b</sup> Department of Electronic Technology, UPV/EHU, Plaza Ing. Torres Quevedo 1, 48013, Bilbao, Spain

### ARTICLE INFO

#### Keywords:

EV  
HEV  
HSEM  
SiC  
Power electronics  
Power converter  
Advanced cooling

### ABSTRACT

In recent decades, several factors such as environmental protection, fossil fuel scarcity, climate change and pollution have driven the research and development of a more clean and sustainable transport. In this context, several agencies and associations, such as the European Union H2020, the United States Council for Automotive Research (USCAR) and the United Nations Economic and Social Commission for Asia (UN ESCAP) have defined a set of quantitative and qualitative goals in terms of efficiency, reliability, power losses, power density and economical costs to be met by next generation hybrid and full electric vehicle (HEV/EV) drive systems. As a consequence, the automotive electric drives (which consists of the electric machine, power converter and their cooling systems) of future vehicles have to overcome a number of technological challenges in order to comply with the aforementioned technical objectives. In this context, this paper presents, for each component of the electric drive, a comprehensive review of the state of the art, current technologies, future trends and enabling technologies that will make possible next generation HEV/EVs.

### 1. Introduction

In this decade, environmental protection and alternative green energies have become one of the main concerns for social and political agents and for the scientific community due to a number of factors, such as greenhouse gas (GHG) emissions, fossil fuels scarcity and their price volatility, or high pollution in modern cities. These factors are accelerating the development of more efficient, sustainable and renewable energy systems [1–6]. Transportation is one of the sectors that most contribute to GHG emissions, producing approximately the 27 % of the total [7].

Within the transportation sector (air, rail and road transport), road transport accounts for the 75 % of transport GHG emissions [2]. Nowadays, population is growing at a remarkable rate. According to

Ref. [8], the world population will rise up to 9.8 billion in 2050, which supposes an increase of 30 % with regard to 2017 population (7.6 billion). As a consequence, the number of road vehicles is expected to be of around 2 billion in 2050 [9]. In this context, road vehicle electrification becomes crucial in order to overcome the aforementioned societal and environmental issues. This last is forcing the research and development of novel concepts and innovations to make electric vehicles (EV) and hybrid electric vehicles (HEV) more efficient, reliable and safe at an affordable cost [1].

Nowadays, there is a great number of original equipment manufacturers (OEMs) producing EVs, HEVs and fuel cell (FC) vehicles (Table 1). Battery powered and Plug-in hybrid EV stock surpassed 2 million vehicles in 2016 [10]. The EV market beat a new record in 2016, with over 750 thousand sales around the world [10], leading to

**Abbreviations:** Al-Cap, Aluminium Electrolytic Capacitor; BJT, Bipolar Junction Transistor; CoFe, Cobalt-Iron; CuBe, Copper-Beryllium; CuZr, Copper-Zirconium; DC, Direct Current; DOE, U.S. Department of Energy; EMI, Electromagnetic Interference; ESR, Capacitor parasitic resistance; ESL, Stray Inductance; EV, Electric Vehicle; FC, Fuel Cell; FOC, Field Oriented Control; GaN, Gallium Nitride; GHG, Greenhouse Gas emissions; HEV, Hybrid Electric Vehicle; HSEM, High Speed Electric Machine; ICE, Internal Combustion Engine; IGBT, Insulated Gate Bipolar Transistor; IM, Induction Machine; JBD, Junction Barrier Diode; JFET, Junction Field-Effect Transistor; MLC-Cap, Multi-layer Ceramic capacitor; MPPF-Cap, Metallized Polypropylene Film Capacitor; MOSFET, Metal-oxide-semiconductor Field-effect transistor; NREL, National Renewable Energy Laboratory; PMSM, Permanent Magnet Synchronous Machine; PWM, Pulse Width Modulation; RBS, Regenerative Braking System; SBD, Solar Electric Vehicle (SEV), Schottky Barrier Diode; SiC, Silicon Carbide; SiFe, Silicon-iron; SRM, Switched Reluctance Machine; SVM, Space Vector Modulation; SynRM, Synchronous Reluctance Machine; TE, Thermoelectric Cooling; THD, Total Harmonic Distortion; TIM, Thermal Interface Material; USCAR, United States Council for Automotive Research; UN ESCAP, United Nations Economic and Social Commission for Asia; WGB, Wide Bandgap

\* Corresponding author.

E-mail addresses: [iraide.lopez@ehu.es](mailto:iraide.lopez@ehu.es) (I. López), [edorta.ibarra@ehu.es](mailto:edorta.ibarra@ehu.es) (E. Ibarra), [asier.matallana@ehu.es](mailto:asier.matallana@ehu.es) (A. Matallana), [jon.andreu@ehu.es](mailto:jon.andreu@ehu.es) (J. Andreu), [inigo.kortabarria@ehu.es](mailto:inigo.kortabarria@ehu.es) (I. Kortabarria).

<https://doi.org/10.1016/j.rser.2019.109336>

Received 17 April 2018; Received in revised form 15 May 2019; Accepted 9 August 2019

Available online 23 August 2019

1364-0321/ © 2019 Elsevier Ltd. All rights reserved.

**List of symbols**

$f_e$	Electric frequency
$p$	Pole number
$P_D$	Total Power Dissipation
$P_{mech}$	Mechanical Power
$R_{c-s}$	Case to heat sink thermal resistance
$R_{j-c}$	Junction to case thermal resistance
$R_{s-a}$	Heat sink to ambient thermal resistance
	Thermal resistance

$T_a$	Ambient Temperature
$T_c$	Case Temperature
$T_j$	Junction Temperature
$T_s$	Sink Temperature
$T_{mech}$	Mechanical Torque
$t_{d,on}$	Turn on delay
$t_{d,off}$	Turn off delay
$V_{DSsat}$	Collector source saturation voltage
$V_{GSsth}$	Gate threshold voltage
$\omega_{mech}$	Mechanical speed

an increase of 33% compared to 2015 [11]. As it can be seen in Fig. 1, China is the country with the largest electric car stock, with the United States in a second place. According to a number of agents, the future market evolution in the following years is promising, and some forecasts expect a global EV stock of 20 million of units in 2020 (Fig. 2). However, the current global electric car stock corresponds to just 0.2% of the total number of passenger light-duty vehicles in circulation [10]. Considering that the previous forecasts can be fulfilled as long as they

**Table 1**

Example of electrified vehicles on the market, including their configuration, machine technology and power ratings.

Model	Year	Vehicle	Config.	Motor	Power (kW) Total/ Electric
Audi	2009	Q5 Hybrid	Hybrid	PMSM	182/40
BMW	2014	i8	Hybrid	PMSM	265/96
BYD	2008	F3DM	Plug-in Hyb.	PMSM	125/75
Honda	2009	Insight	Hybrid	PMSM	83/10
Honda	2001	Civic	Hybrid	PMSM	69/10
Audi	2009	Q5 FCEV	Fuel cell	IM	80
Ford	2000	Ford P2000	Fuel cell	IM	67
Honda	2008	FCX Clarity	Fuel cell	PMSM	100
Hyundai	2013	ix35 FCEV	Fuel cell	IM	100
Mercedes	2010	Clase B F-Cell	Fuel cell	PMSM	100
Toyota	2015	Mirai	Fuel cell	PM	113
BMW	2013	i3 BEV	Electric	PMSM	125
BYD	2014	E6	Electric	PMSM	90
Citroën	2011	C-Zero	Electric	PMSM	47
Citroën	2016	E-Mhari	Electric	PMSM	50
Ford	2011	Focus Electric	Electric	PMSM	107
Kia	2014	Soul EV	Electric	PMSM	81.4
Land Rover	2013	Defender	Electric	SRM	70
Mercedes	2014	SLS AMG ED	Electric	PMSM	550
Mercedes	2014	Clase B ED	Electric	PMSM	132
Mitsubishi	2009	i-MIEV	Electric	PMSM	47
Nissan	2010	Leaf	Electric	PMSM	80
Peugeot	2010	iOn	Electric	PMSM	49
Peugeot	2014	Partner Electric	Electric	PMSM	49
Porsche	2020	Mission E	Electric	PMSM	440
Renault	2001	Kangoo I	Electric	PMSM	from 22 up to 29
Renault	2011	Kangoo ZE	Electric	PMSM	44
Renault	2011	Fluence ZE	Electric	PMSM	70
Renault	2012	Twizy	Electric	PMSM	8
Renault	2012	Zoe	Electric	PMSM	65
Smart	2011	Fortwo ED	Electric	PMSM	55
Tazzari	2009	EM1	Electric	IM	20
Tazzari	2009	Zero Classic	Electric	IM	20
Tesla	2011	Roadster	Electric	IM	185
Tesla	2012	Model S	Electric	IM	from 235 up to 568
Tesla	2015	Model X	Electric	IM	from 193 up to 375
Think	2008	Think City	Electric	IM	34
Toyota	2012	RAV4 EV	Electric	IM	115
Volkswagen	2014	e-Golf	Electric	PMSM	85
Volkswagen	2013	e-UP	Electric	PMSM	60

PMSM: Permanent Magnet Synchronous Machine.

IM: Induction Motor.

SRM: Switched Reluctance Machines.

meet all the requirements from which they have been based, it is more realistic to define a scenario with an electrified vehicle increase between 9 million and 15 million units by 2020 [11].

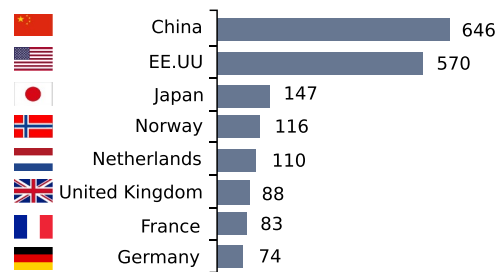
In order to achieve all these market objectives, it becomes clear that it is necessary to provoke a change in the society and make the EV an attractive road transport alternative. From the end user point of view, the main technical aspects that are considered to decide whether or not purchase an EV or HEV are vehicle power, efficiency, maximum speed, dynamic response, reliability, autonomy and, last but not least, economical costs. All these items are related with the vehicle electric drives, which include electric machines, power electronics and their respective cooling systems. From a technical point of view, significant advances will be required in order to achieve the required cost reductions for the popularization of HEV/EV technologies.

Historically, advances in transport drives have been conducted following progressive steps. From 1995 to 2005, electric drive systems research targets focused on the development of basic automotive components (integrated electric motor drives and power modules with maximum junction temperatures of 125 °C and switching frequencies between 2 kHz and 10 kHz) [12]. From 2005 to 2015 great efforts were conducted in order to achieve higher junction temperatures (150 °C), high switching frequency operation (up to 12 kHz) and integrated motor and power electronics [12]. Regenerative braking systems (RBS), which allow recharging the energy source by feeding back energy from the electric machine during braking, have also been developed and extensively investigated over the last years, as their implementation can improve fuel efficiencies between 30% and 40% for HEVs [13], and driving range can be extended between 8% and 25% for EVs [14]. Relevant examples of recent investigations aiming to improve regenerative braking include the dynamic detection of the lowest speed threshold at which electric braking is effective [15], control algorithms for independent regenerative braking torque-vectoring on vehicles with in-wheel machines [16,17], or investigations where motor and hydraulic braking forces are coordinated [18].

Currently, the U.S Department of Energy (DOE) identifies a number of technical aspects in the report called *EV Everywhere* [19]. Based on the aforementioned features required by the consumers, *EV Everywhere* also defines a set of goals and technical targets. In this context, Table 2 shows quantitatively power density, efficiency and cost targets for future HEV/EV electric drives. Other national and international programmes, adopted by each community or country, have also similar qualitative and quantitative targets to be reached by the future electric propulsion technologies. Among them, Horizon 2020 [20], the United States Council for Automotive Research (USCAR) [21] and the United Nations Economic and Social Commission for Asia (UN ESCAP) [22] represent global HEV/EV technology trends, as they cover Europe, North America and Asia. According to these programmes, the expected improvements in future EV propulsion systems can be summarized as [20–22]:

1. Increase of torque production capability of the electric machine by 30% and speed by 50%.
2. Reduction of 50% on motor losses.

Ranking of countries by VE stock (thousand of units, 2016)



Ranking of countries by market share by total fleet (% , 2016)

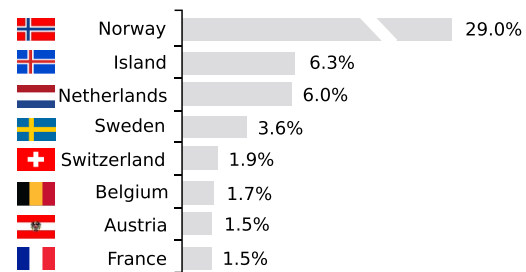


Fig. 1. Electric vehicle market in 2016 [10].

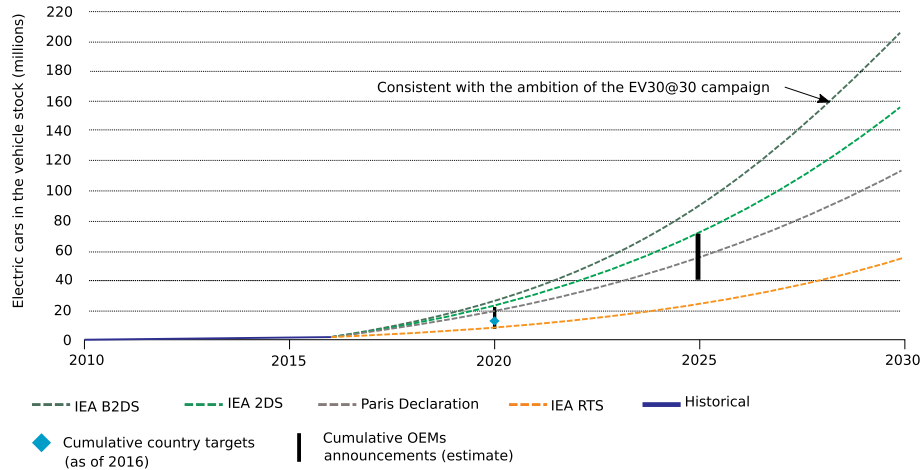


Fig. 2. Deployment scenarios for the stock of electric cars to 2030 forecast by relevant agents [10].

Table 2

Current status and future targets for EV drive main components (electric machine and power electronics) in terms of power density, efficiency and costs (from Refs. [23,24]).

Characteristic	Electric motor			Power electronics		
	2010	2015	2020	2010	2015	2020
Specific power (kW/kg)	1.2	1.3	1.6	10.8	12	14.1
Power density (kW/l)	3.7	5.0	5.7	8.7	12	13.4
Efficiency (%)	90	92	93	91	94	97
Cost (\$/kW)	11.1	7	4.7	7.9	5	3.3

- Power density increase of 50% in power converters and, at the same time, reduction of power converter losses by 50%.
- Overall efficiency optimization of 20%.
- Powertrain system (motor, power converter and energy source) weight and volume reduction of 40%.
- Costs reductions (four times reduction) on electric machine and power electronics.
- Simplification of the thermal management systems using on-board coolants with minimal additional components as possible.

As a consequence of these specific targets, the main elements to be integrated in future HEV/EV electric drives will face a number of challenges that should be overcome. In this paper, the aforementioned challenges are identified, and technological solutions required to constitute these future drives are also thoroughly reviewed. In this sense, section 2 overviews vehicle electrification architectures and lists the enabling technologies for the required future innovations, section 3 focuses on the electric machine and torque control challenges and solutions, while sections 4 and 5

determine power converter and cooling system challenges and solutions, respectively.

## 2. EV and HEV propulsion architectures and enabling technologies for next generation drives

In general terms, the main electric vehicular architectures that compete with internal combustion engine (ICE) vehicles are: battery powered electric vehicles (EV), hybrid electric vehicles (HEV), fuel cell vehicles (FC), fuel cell hybrid electric vehicles (FCHEV) and hybrid solar electric vehicles (HSEV).<sup>1</sup> Fig. 3 shows these architectures, while a comparative analysis of ICE vehicle and electrified vehicles are summarized in Table 3.

One of the main differences between those architectures relies on the energy source. For example, EVs and HEVs rely on batteries, while FCs rely on hydrogen fuel cell stacks (zero emission vehicle, only emits water and heat). FC supplies a constant power, but it does not adapt properly to a rapid change of power demand, being its major application slow speed vehicles (buses, trams, etc) [29,30]. However, a FCHEV configuration can be obtained using a FC as the main energy source and battery as an additional storage system. Here the operation range and speed are increased at the expense of the modification of the powertrain. In this context, some manufacturers such as Honda, Toyota and Hyundai manufacture high performance FCHEVs [30]. With the aim of extend the range autonomy and reduce the environmental impact, there are also architectures based on solar panels installed on the top of the vehicle (HSEVs), which combine the benefits of solar energy (available,

<sup>1</sup> Considering current technology, solar vehicles without hybridization do not have enough autonomy for current mobility requirements.

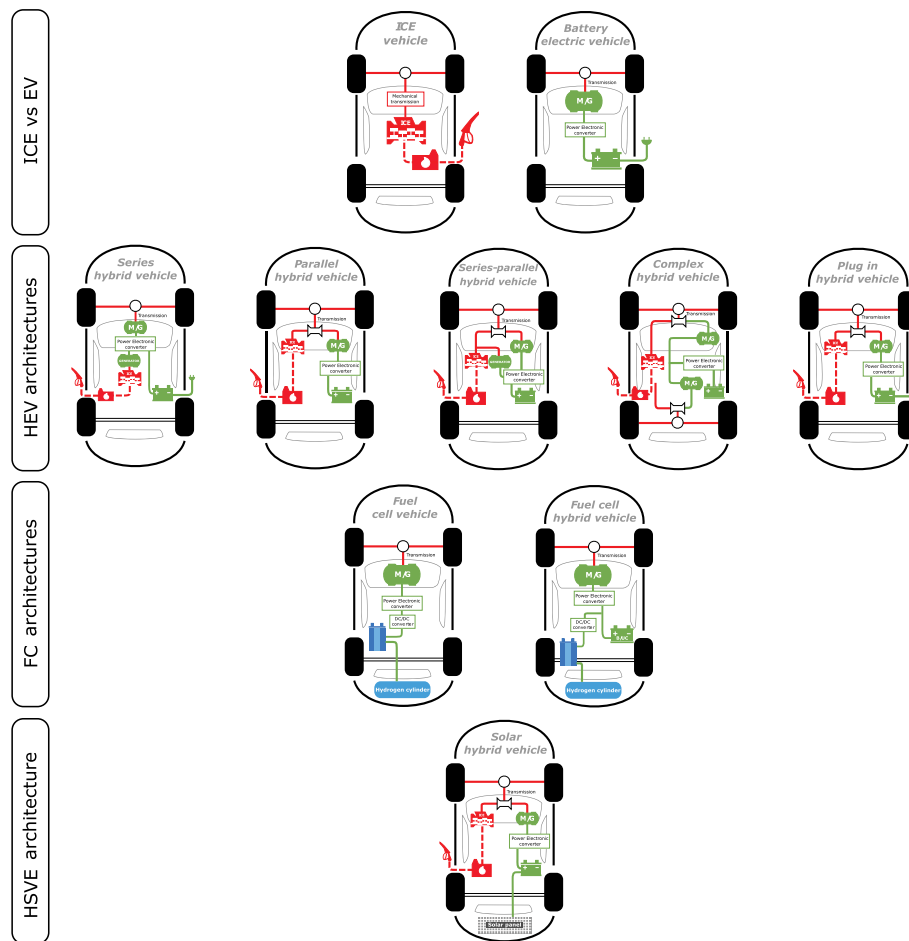


Fig. 3. Architecture and configuration of ICE and EV, FC and HEV (adapted from Ref. [1]).

sustainable, renewable and clean) with the HEV characteristics, obtaining a fuel-efficient vehicle [29,31,32].

Although a number of vehicular topologies can be found in the literature, the majority of manufacturers rely on EVs and/or HEVs. EVs have a simple structure where energy flows from or to the battery through the bidirectional power converter (Fig. 3). On the other hand, and depending of its internal configuration, hybrid vehicles can be classified as series HEV, parallel HEV, series-parallel HEV, complex HEV and plug in HEV [1], which differences rely on the way energy flows from the storage sources of energy [32–34].

With independence of the vehicular architecture, the electric drive (power converter and electric machine) is the core of all these electrified powertrains (Fig. 3). The development of next generation green vehicles based on advanced electric drives requires to focus on the following aspects: cost reduction, efficiency improvement and achievement of high power densities [35]. The key enabling technologies that will improve the aforementioned features on electric machines can be summarized as [12,35–39]:

- Cost reduction: (a) usage of new magnet materials without rare earths and heavy rare earths and (b) simplification of the cooling system (air cooling is considered among other solutions).
- High efficiency: (a) development of high performance alloys, such as magnetic steels and copper alloys and (b) the design of machines with low copper and iron losses.
- High power density: (a) increase of the electric machine operation speed and (b) high performance cooling for increased power

capabilities.

On the other hand, the following enabling technologies must be considered for future power converters [12,35–38]:

- Cost reduction: (a) revolutionary and/or evolutionary changes to designs or manufacturing techniques and (b) simplification of the cooling system (as in the case of the electric motor, air cooling is considered as a possibility).
- High efficiency targets, with the implementation of wide bandgap (WBG) semiconductor technology with low switching losses.
- High power density targets, (a) by introducing WBG technology including advanced packaging and (b) by implementing optimum thermal management.

Note that some of the requirements lead to opposite design concepts. For example, regarding the cooling system, a trade off between simplification (cost reduction) and thermal management optimization (high power density targets) must be followed, being this particular aspect challenging for researchers. The same applies to non rare-earth based machine technologies and power density targets.

In the following sections, a deep and extensive study of the core components and technologies of electric drive is performed, which include the electric motor, the bidirectional converter and the thermal management, pointing out both the advantages and disadvantages of each technology and the new challenges that these entail to get the future technical goals.

**Table 3**  
Characteristic of ICE vehicle, EV, FC and HEV [25–28].

Feature	ICE vehicle	EV	HEV	Plug-in HEV	FC
Propulsion System	ICE based	ED based <sup>(1)</sup>	ICE & ED based	ICE & ED based	ED based
Energy storage	Fuel tank	Battery Ultra capacitor Flywheel	Fuel tank Battery Ultra capacitor Flywheel	Fuel tank Battery Ultra capacitor Flywheel	Fuel cell tank Battery Ultra capacitor Flywheel
Energy source	Petrol	Electric	Petrol & electric	Petrol & electric	Hydrogen
Energy source infrastructure	Refueling station	Charging station	Refueling station	Charging station & refueling station	Hydrogen refiner & refueling station
Well-to-tank <sup>(2)</sup>	88.0%	37.0%	88.0%	-( <sup>3</sup> )	58.4%
Tank-to-wheel <sup>(2)</sup>	12.1%	83%	22.3%	-( <sup>3</sup> )	46.6%
Well-to-wheel <sup>(2)</sup>	10.6%	31.3%	19.6%	-( <sup>3</sup> )	27.2%
Commercialized	Yes	Yes	Yes	Partially	No
Smooth operation <sup>(4)</sup>	No	Yes	Yes	Yes	Yes
Emissions	Very high	No	Very low	Low	Ultra low
System complexity	Very low	low	Medium	High	Very high
Bulky	Yes	No	Yes	Yes	No

<sup>(1)</sup> ED based: Electric Drive system based.

<sup>(2)</sup> Approximate values. Gasoline has been considered as fuel for hybrid configurations.

<sup>(3)</sup> These numbers will highly depend on the specific vehicle and will be between HEV and EV values.

<sup>(4)</sup> Regarding torque ripple.

**Table 4**  
Comparison of the main features of prototype and marketed PMSM, PM-assisted SynRM, IM and SRM technologies for HEV/EV applications.

General features	PMSM	PM-assist. SynRM	IM	SRM
Fault tolerance	✓	✓	x	✓
Robustness	x	x	✓	✓
Reliability	moderate	moderate	high	moderate
Wide speed range <sup>(1)</sup>	✓	✓	x	✓
Close loop control simplicity	✓	✓	✓	✓
Preferred torque control algorithms	FOC, DTC	FOC, DTC	FOC, DTC	DITC, ADITC, IDITC
Field weakening operation capabilities	✓	✓	✓	✓
Torque ripple	low	low	low	very high
Acoustic noise	low	low	low	moderate
Maximum power limitation by technology	virtually not <sup>(2)</sup>	virtually not <sup>(2)</sup>	virtually not <sup>(2)</sup>	yes <sup>(3)</sup>
Power conversion topologies	VSI	VSI	VSI	Asymmetric H-Bridge
Efficiency and power densities	PMSM	PM-assist. SynRM	IM	SRM
Typical efficiencies at constant torque region <sup>(4)</sup>	91.3–95.8%	87.0–93.0%	79.0–86.0%	85.1–89.0%
Power densities of current technologies (kW/l) <sup>(5)</sup>	3.3–10.2 kW/l	6.8 kW/l	2.5 kW/l	2.6–4.5 kW/l
Costs	PMSM	PM-assist. SynRM	IM	SRM
Overall technology costs	high	medium	medium	low
Relative material costs	10/10 <sup>(6)</sup>	4.8/10 <sup>(7)</sup>	5.9/10 <sup>(6)</sup>	3.1/10 <sup>(6)</sup>

<sup>(1)</sup> Maximum mechanical speeds of around 5000–8000 rpm in the current automotive market, with a number of high speed drives with maximum speeds up to 16000 rpm.

<sup>(2)</sup> High power machines that cover the light and heavy duty EV requirements can be manufactured using IM and synchronous technologies.

<sup>(3)</sup> As in SRM technology only one phase is responsible of torque production at each instant, virtually no SRMs for EV applications with powers higher than 100 kW has been found in the literature.

<sup>(4)</sup> Efficiency ranges and power densities of each technologies have been obtained from EV machine designs studied in Refs. [57,79–90].

<sup>(5)</sup> Data obtained from prototypes and real motors analysed in Refs. [76,91].

<sup>(6)</sup> The detailed cost analysis has been carried out in Ref. [79] using comparable PMSM, IM and SRM machines manufactured with current technologies and targeting medium speed EV machine applications with a nominal power of 50 kW. No manufacturing costs included. Prices of 2008 and 2010 considered for copper and magnets. The exact material costs for PMSM, IM and SRM where 242,17 \$, 143,80 \$ and 74,16 \$, respectively.

<sup>(7)</sup> According to Ref. [92] and compared to the second generation Prius motor. No manufacturing costs have been considered, which can be significant in PM-assisted SynRMs due to their complex rotor structure.

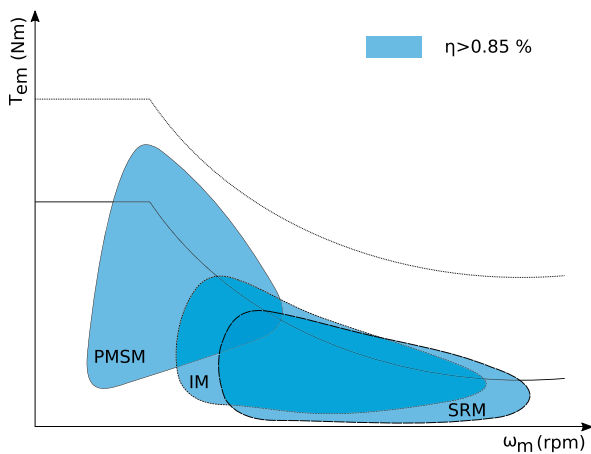


Fig. 4. Qualitative efficiency map for PMSM, IM and SRM [76].

### 3. Next generation electric machines for EV and HEV propulsion systems

#### 3.1. Current electric machine technologies: overview and comparison of most relevant features

The most established EV and HEV electric machine technologies are, by far, Permanent Magnet Synchronous Machines (PMSM) and Induction Machines (IM) [40]. As it can be derived from Table 1, PMSM [41–46] are the preferred option in current EV and HEV vehicles. The main reason is their high efficiency and superior power density, which is particularly a critical factor in HEVs (due to their tight space constraints). Specially, Interior PMSMs are employed, as the additional reluctant torque allows to achieve higher power density than their Surface Mounted PMSM counterparts [41]. However, technologies that do not rely on rare-earth based magnets are gaining popularity [2,41,47], due to the scarcity, price fluctuations and high costs associated with these materials (neodymium and, in lower quantities, dysprosium and terbium) [47–51]. Among them, the mature squirrel cage IM [52–56] has a real market penetration (Table 1) in the automotive industry, while other electric machine technologies, such as Ferrite based Permanent Magnet Assisted Synchronous Reluctance Machines (PM-assisted SynRM) [57–61] and Switched Reluctance Machines (SRM) [62–66] are gaining attraction from the scientific community.

In PM-assisted SynRMs the rotor is manufactured in a way that the asymmetry between the  $d$ - and  $q$ -axes is maximized. Thanks to this, the reluctant torque of the electric machine is maximized, allowing to achieve power densities of around 75% of an interior PMSM for the same size and liquid cooling technology [67]. As a drawback, the ferrite-PM-assisted SynRM machine may suffer from demagnetization at low temperatures, which can be avoided or minimized by a proper design or by preheating the magnets before machine start [58,68]. This type of machine is being extensively researched [58,60,69] and, although there are virtually no commercial solutions equipped with this technology [47], it represents a promising alternative for the future.

SRMs have a double salient structure (saliency in both stator and rotor) and no magnets nor windings in the rotor [70]. This saliency is used for electromagnetic torque production, requiring a specific control approach that takes into account the non-linearities of the machine [71]. As opposite to synchronous and induction machines, SRMs require an H-bridge converter topology (generally in asymmetric configuration) instead of a common Voltage Source Inverter (VSI) [72]. SRMs exhibit a number of advantages such as simple structure, flexibility of control, high efficiency, lower cost and intrinsic fault tolerance [62,72]. Although SRMs can be considered as a low cost solution for EV and HEV applications, they have significant disadvantages that must be

considered, such as high torque ripple, medium power density, high DC bus current ripple, high acoustic noise and high electromagnetic emissions (EMI) [72,73].

The 6/4 pole SRM can be considered as the standard configuration for EV applications [74]. However, new design approaches that partially overcome the aforementioned drawbacks are being currently researched [63–65,75]. Generally speaking, the main drawbacks of these advanced structures are their added manufacturing complexity and additional costs. According to Ref. [47], SRMs are now being introduced into vehicle prototypes. Land Rover and Toyota (in partnership with Renault-Nissan) are currently working on SRM drives (Table 1).

Quantitative and qualitative comparisons of the most relevant machines (PMSM, PM-assisted SynRM, IM and SRM) can be found in the scientific literature [76–85]. Table 4 collects both general features and quantitative values of each technology. It becomes clear that the PMSM technology is superior regarding power density. Although PM technology shows the best efficiencies below base speed, the common operation range of the target electric vehicle must be considered to determine the solution that gives a better overall efficiency during the life-cycle of the vehicle. Generally speaking, in efficiency terms PMSM could be preferred for urban driving, as extra current is required at field weakening operation (high speeds), while IMs and SRMs would be more efficient for high speed sport cars (Fig. 4).

Regarding cost and simplicity, SRM technology could be considered the best option, being this a critical aspect in the automotive industry. However, the disadvantages associated with its technology (high torque ripple, noise, vibrations) seem to favour the IM technology, as it can be confirmed from the market penetration of each technology (Table 1).

From the reviewed literature [76–85], it can be concluded that the suitability of each technology depends on the specific context of a given propulsion system. Thus, it is not possible to determine the absolute superiority of one technology over others and a technological decision must be conducted after analysing a number of factors for a given application. In this context and once the most significant requirements of a given EV or HEV vehicle are defined (torque requirements, power, speed, gearbox characteristics, etc.), the main features that must be compared to select the proper electric machine technology for the particular application can be summarized as [76]:

- Required installation space and tolerable machine weight (or power density).
- Specific reliability requirements.
- Overall efficiency within the whole operation range.
- Torque vs speed characteristic.
- Overload capability of the drive.
- Overall cost, including materials and manufacturing.

Although PMSM, IM, PM-assisted SynRM and SRM technologies have attractive aspects for their inclusion in EV propulsion system drives, the vast majority of EV and HEV manufacturers rely on synchronous or induction machines (Table 1). Up to 2010, 56% of commercial electrified vehicles had PMSMs installed, while 29% had IMs installed. SRM technology had a market penetration below 1%, being the trend towards PMSMs and IMs clear for the next years [40]. Thus, in the following this article will focus on the aforementioned motor technologies.

##### 3.1.1. Electrified vehicle drive phase-number

Three-phase technologies have become the standard in light to medium weight vehicle propulsion systems based on synchronous and IM machines, while multiphase approaches are generally used for heavy vehicles (due to power constraints) and for in-wheel applications [81,93] where the highest possible power density is preferred [93]. Multiphase technologies include a number of benefits that could also be exploited in light and medium vehicles, such as power splitting,

increased fault tolerance, high efficiency, high power density and lower torque ripple than three-phase machines [94–96]. Among these technologies, dual three-phase machines [97–100] can be highlighted, because they allow the usage of independent three-phase voltage source inverters providing a high fault tolerance. Other multiphase configurations with an odd number of phases and star connection can be also considered for EV and HEV applications [94,95].

### 3.2. High speed electric machines for vehicle propulsion

#### 3.2.1. Trends on high speed operation

With independence of the machine technology, design trends for next generation EV and HEV propulsion systems (section 1) include the increase of the operation speed of such machines ( $\omega_{mech}$ ), as the same power ( $P_{mech}$ ) can be delivered producing lower torque ( $T_{em}$ ) (1) and, consequently, requiring a smaller and lighter machine [83].

$$P_{mech} = T_{em}\omega_{mech}. \quad (1)$$

This trend is a consequence of the volume constraints of vehicles, specially in HEVs, where both electric and internal combustion motors must share a reduced space. Weight reduction also improves the efficiency and autonomy of the vehicle, which is a critical point for the adoption of EV technologies. Following this trend, Toyota has approximately doubled its Interior PMSM drive mechanical speed from 2nd generation to 3rd generation Prius, i.e., from 6000 rpm (launched in 2004) to 13900 rpm (launched in 2010), featuring both machines the same nominal power of 50 kW [47]. This trend is also being followed by other manufacturers such as Chevrolet, as the IPMSM of the Chevrolet Volt has been designed to reach a maximum speed of 8810 rpm, which represents a significant increase when compared to its predecessor the Chevrolet Spark (exhibiting a maximum speed of 4500 rpm) [106].

A great amount of medium speed EV electric drives with maximum speeds in the range of 5000–8000 rpm can be found in the manufacturers' portfolio (Remy, EVO, Yasa, TM4, Parker, etc.). As stated in Refs. [39,105], motors can be considered as high speed electrical machines (HSEM) if they operate at mechanical speeds beyond 10000 rpm. Table 5 shows various current commercial, prototype and conceptual

high speed machines intended for EV and HEV applications. The great majority of these HSEMs have a maximum mechanical speed between 10000 rpm and 15000 rpm. However, considering future drive volume reduction targets (section 1), it is expected that in the near future the mechanical speeds of these machines will be much higher than 15000 rpm [83,84].

This high speed operation implies a number of technological challenges that must be overcome in order to achieve a satisfactory mechanical behaviour and torque regulation of the machine along the whole operation range of the drive. This problematic is thoroughly studied in the following.

#### 3.2.2. Electromechanical HSEM design aspects

Although HSEMs have been commonly used in a number of applications, the design of HSEMs that fulfill the high torque and fast dynamic requirements of an EV or HEV can be challenging. A number of machine design aspects must be taken into account to successfully implement an HSEM. On the one hand, mechanical constraints, such as a proper bearing design must be considered. Vibrations and noise can be problematic at such high speeds [83,84]. Additionally, the high speed machine should be linked to a magnetic gear (MG) [84,107] with a high transmission ratio.

The choice of the air-gap is also of great importance [108]. A good rotor cooling at high speed operation requires that the radial clearance gap between the motor stator and rotor must be relatively large [84]. However, this would decrease significantly the performance of the machine, as the flux linkage is reduced.

In PMSM technologies (particularly in surface mounted machines) alternative rotor magnet mounting configurations, such as structures with partially inset magnets [109,110] must be considered in order to avoid magnet detach due to high centrifugal forces. Additionally, retaining rings [111] can be considered at the cost of increasing the machine air-gap size. The amount of rotor poles must be also carefully selected, because a great number of poles implies a high stator frequency, which has a great impact in the magnetic losses of the machine [112,113].

For high speed IMs, copper alloys, such as copper-zirconium (CuZr),

**Table 5**

High speed electric machine examples for EV and HEV applications. If not cited, the information has been obtained from the manufacturer product documentation.

Model/Reference	Type	Mech. speed (rpm)	Poles	Power (kW)
Tesla Roadster	IM	14000	4	185
Tesla model S <sup>(1)</sup> [83]	IM	16000	4	150
Conceptual design (presented in Ref. [101])	IM	40500	2	40
Toyota Prius 3rd generation [47]	IPMSM	13900	8	50
Nissan LEAF 2012 [102]	IPMSM	10390	8	80
EVO AF-125 <sup>(2)</sup>	SM-PMSM	12000	n.s. <sup>(3)</sup>	85
Remy HVH250 standard <sup>(4)</sup>	PMSM	10600	n.s.	82
TM4 HSM20-MV80	PMSM	11750	n.s.	40
TM4 HSM60-MV255	PMSM	12500	n.s.	85
Prototype (presented in Ref. [83])	SM-PMSM	22000	2 <sup>(7)</sup>	20
Prototype (presented in Ref. [84]) <sup>(5,6)</sup>	SM-PMSM	40500	2 <sup>(7)</sup>	40
Symemo machine (prototype [103]) <sup>(8)</sup>	PM-assisted SynRM	12000	6	51
Conceptual design (presented in Ref. [104])	PM-assisted SynRM	14000	8	64
Conceptual design (presented in Ref. [105]) <sup>(9)</sup>	Ferrite BLDC	100000 <sup>(10)</sup>	2	40

<sup>(1)</sup> 600 V IGBT inverter with air cooling on both machine and power converter. Multiple machine vehicle architecture.

<sup>(2)</sup> Axial flux.

<sup>(3)</sup> n.s.: not specified by the manufacturer.

<sup>(4)</sup> With High Voltage Hairpin (HVH) stator.

<sup>(5)</sup> The usage of a Magnetic Gear (MG) of 1:26 gear-ratio is proposed in order to achieve the target maximum speed with reduced maintenance, improved reliability, reduced acoustic noise, and inherent overload protection.

<sup>(6)</sup> The inverter operates with a switching frequency of 18 kHz.

<sup>(7)</sup> One pole-pair configuration is selected in this particular case in order not to excessively increase the electric frequency and keep the magnetic losses as low as possible.

<sup>(8)</sup> Tested in laboratory under standardized driving cycles.

<sup>(9)</sup> It can use MG or a single gear transmission system.

<sup>(10)</sup> Being the rated speed 30000 rpm.

copper-beryllium (CuBe) and copper-aluminium oxide (CuAl<sub>2</sub>O<sub>3</sub>) can be used to implement machine rotor and improve machine performance [39]. As a drawback, copper conductivity is reduced. The usage of solid rotors should also be considered [39].

In both PMSMs and IMs, magnetic losses should be minimized by design [114]. In this sense, high performance electrical steels with low core losses, such as cobalt-iron (CoFe) and silicon-iron (SiFe) can be used for iron loss reduction [39]. Finally, torque ripple should be reduced by means of a highly sinusoidal air-gap flux design in order to facilitate torque control at high speeds and reduce losses [39,84].

Once these design and manufacturing aspects have been considered, an adequate control approach must be set in order to properly operate the machine at high speeds.

### 3.3. Torque control in HSEMs

#### 3.3.1. Efficiency optimization and field weakening control

Being a battery connected system, the main target of the electric machine controller is to produce the required torque tracking the maximum efficiency points at a given operation condition [44,103]. High magnetic saturation is a very common feature in EV electric machines, because a compact design is preferred due to vehicle space constraints [115,116]. However, modern torque control strategies can deal with this issue, ensuring an optimal control that minimizes the machine power losses, even under high non-linearities [44,103,117].

Another direct consequence of high speed operation is the extension of the field weakening and, in some cases, deep field weakening regions. In field weakening operation, the stator voltage limit (due to the DC-link voltage constraints) must be considered and effectively regulated [42,44,103,118]. If this constraint is exceeded, uncontrolled regeneration occurs [103], limiting the maximum speed achievable for the electric drive.

This implies the need of reliable field weakening control strategies that regulate the stator voltage amplitude. This topic has been widely covered in the literature for synchronous and induction machines, leading to a number of robust field weakening regulation approaches [44,103,119,120]. However, as the speed increases, the lower number of control samples per stator electric period can make a proper field weakening control challenging.

#### 3.3.2. Current regulation challenges in HSEMs

Although a number of torque regulation schemes can be found in the scientific literature, Field Oriented Control (FOC) is the most commonly used one and it is widely accepted for the industry for synchronous and induction machines control [53,121–123]. This is mainly due to its good dynamic performance, moderate computational burden and operation of the power converter at a fixed switching frequency [124].

In general, a multi-polar approach electric machine design is followed in vehicle electrification (Table 5). As a consequence of both high mechanical speed operation and multiple pole design, the electric frequency ( $f_e$ ) that must be synthesized in the stator by the power converter can be very high, as:

$$f_e = \frac{1}{2\pi} \frac{p}{2} \omega_{mech}, \quad (2)$$

being  $p$  and  $\omega_{mech}$  the pole number and mechanical speed (in rad/s) of the electric machine, respectively. Taking into account the discrete nature of the regulators, this implies that machine controllability issues can arise in current regulation due to the following reasons:

- Lack of synchronization between the measurements of the electrical and mechanical parameters required by the torque controller at each control period, i.e., stator currents and rotor position and speed. This must be carefully handled during the controller digital implementation.

- Delays produced by the digital regulator. When FOC (or a similar fixed sampling frequency approach) is used for current regulation, it is not enough to only consider these delays in the design of the current regulators, for example, PI regulators [125]. In Ref. [126] and following a comprehensive discrete-time domain formulation, it has been demonstrated that Park transformations are responsible for introducing instabilities due to such processing delays. The effect of these delays can be corrected, for example, by adding a phase advance to the electrical angle  $\theta_e$  used for the voltage inverse Park transformation [127]. The following compensation must be carried out using the following expression when symmetrical Pulse Width Modulation (PWM) or Space Vector Modulation (SVM) is applied [103,127]:

$$\theta'_e = \theta_e + \frac{3}{2} \frac{p}{2} \omega_{mech} T_s, \quad (3)$$

being  $T_s$  the execution period of the controller. It must be borne in mind that this solution extends the controllable speed range, but has its limitations [127].

- Low fundamental-to-sampling frequency ratios, leading to oscillations or even control instabilities [128,129]. If this number of samples is not high enough to ensure controllability, an increase in the controller and the power electronics execution and switching frequencies can be carried out, or control approaches that include advanced regulators which can cope with this problematic can be employed [126,129–131].

Fig. 5 shows, as an example, how a PMSM with 18 poles losses control due to an insufficient controller sample-time and because no mitigation strategy has been applied.

Although control techniques that mitigate the controllability problems due to high fundamental-to-sampling frequency ratios can be found in the scientific literature, the following points must be taken into consideration:

1. High nonlinearities of electric vehicle machines make the implementation of such high speed control laws extremely difficult [130].
2. Field weakening control strategies could require high sampling rates in order to provide a satisfactory stator voltage constraint control (specially for PM based machines).
3. The fundamental and the PWM harmonic components become close, and torque regulation precision decreases, leading to a high Total Harmonic Distortion (THD) of the synthesized stator voltages and

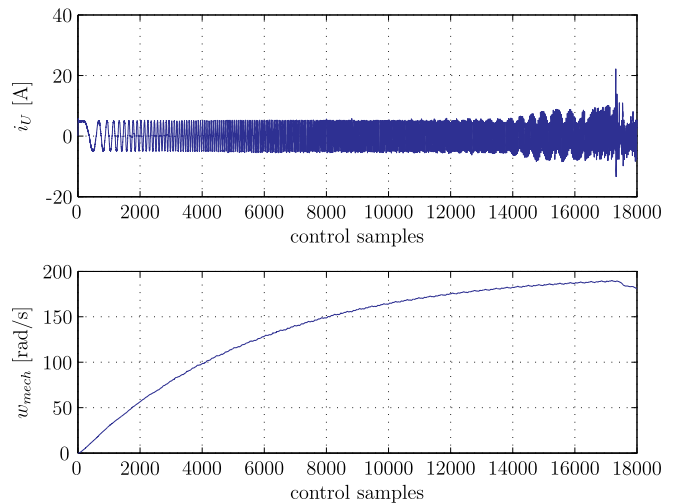


Fig. 5. Example of torque control loss due to insufficient controller execution period of 100  $\mu$ s in a surface mounted PMSM with 18 poles.



currents. As a consequence, machine losses can increase significantly. Another important aspect relies on the fact that DC-link capacitor current ripple should be increased. As a consequence, a capacitor with higher RMS current withstanding capability (which is usually bulkier) could be required.

Taking into account the aforementioned points, it can be concluded that the most effective approaches that can be followed in order to cope with high speed control issues is the combination of the following solutions:

- Include the delay compensation control approach proposed in Ref. [127] in the control structure, ensuring by programming that possible measurement synchronization loss is minimized.
- Increase of the switching frequency of the power converter [128] in order to reduce the fundamental-to-sampling- frequency ratio and improve both torque and field weakening regulation.

This increase on the switching frequency has significant technological consequences, specially in the elements that constitute the power converter, i.e., power semiconductors, driver board, control board, reactive elements and cooling system. In the following, the consequences of this challenges and the technological approaches that overcome them will be thoroughly reviewed.

#### 4. Wide bandgap based power control units for automotive drive systems

The power converter can be considered as the core element of the electric drive, as it is responsible for controlling the bidirectional power flow between the electric machine and the battery pack. Fig. 6 shows the general diagram of an HEV/EV power converter, which, in this particular case, incorporates a three-phase voltage source inverter. This diagram also shows the common layout of an automotive power converter, including its main functional blocks, i.e., power semiconductor devices, driver board, dc-link capacitor(s) and bus bar.

In the following paragraphs, the primary requirements and the major trends of these functional blocks for next generation HEV/EV automotive power converters will be described. The thermal management technology (cold plate in Fig. 6) is also a key element of a power converter. This block will be separately reviewed in section 5.

##### 4.1. Power semiconductors

Power semiconductor devices are the key components in any power electronics system. Their optimization entails improvements in relevant aspects of the electric drive, such as efficiency, reliability, specific mass and volume of power converter, power losses, power density, or quality of synthesized voltage and current waveforms [132–135].

In the particular case of the automotive industry, automotive grade power semiconductors are required for the industrialization of power converters. The automotive grade certificate ensures the quality,

performance and safety of the product under the stringent automotive operation conditions. The Automotive Electronics Council has developed the AEC Q101 (Stress Test Qualification for Discrete elements) standard, which establishes common part-qualification and quality-system standards for automotive power semiconductors in terms of life-cycle, operation temperature, humidity and vibrations.

In general, current automotive power converters rely on the well established and mature silicon (Si) technology [136–138]. However, with regard to the technological and cost targets for next generation HEV/EV drives (section 1), Si exhibits a number of limitations in terms of blocking voltage capability, operation temperature and switching frequency [133,139]. As control of future HSEMs will require to operate at high switching frequencies (section 3.3), the relatively high switching losses of Si devices will reduce drastically the efficiency of power converters, leading to the need of complex and expensive cooling systems [133,140], or even making this technology infeasible for the application. Consequently, the introduction of a new generation of power devices based on wide band gap (WBG) semiconductor materials will be required in future automotive power converters. The larger band gap of WBG materials leads to a lower intrinsic carrier concentration and an increase of the maximum operation junction temperature. Their high thermal conductivity also reduces the thermal resistance of the device [134]. Thus, Si drawbacks could be overcome to a great extent with this technology [135].

Silicon carbide (SiC) and gallium nitride (GaN) are currently considered as the most matured WBG technologies [132–135,141–144]. The high critical field of SiC and GaN allows to operate at higher voltages when compared to Si devices [145,146]. Likewise, GaN has higher electron mobility than SiC, meaning that, theoretically, GaN devices are the best suited for high switching frequency operation. However, SiC exhibits a higher thermal conductivity. Consequently, SiC devices could be preferred for high power density applications [145]. Although GaN technology shows superior features than SiC in most parameters, its lower thermal conductivity becomes a big challenge for system designers [147]. As a summary, Table 6 shows a comparison of the most relevant physical parameters of Si, SiC and GaN materials.

In the following, SiC and GaN diode and active switch semiconductors are reviewed. The requirements to be met for them in automotive electric drives will be discussed.

##### 4.1.1. SiC devices

As in silicon technology, there are different SiC devices, among which stand out SiC based Schottky barrier diodes (SBD) and junction barrier diodes (JBD), PiN diodes, JFETs, BJTs and MOSFETs, which have been available in the market since some years ago. Regarding diodes, the junction knee voltage of SiC PiN diodes makes them ineffective for blocking voltages below 3.3 kV [140,148]. Likewise, the reverse recovery current of SiC PiN devices results in large reverse recovery losses [148]. Consequently, SiC Schottky diodes could be preferred for automotive applications. Both SBD and JBD diodes are well suited for applications in which high switching frequency operation is required, and they also match perfectly as freewheeling diodes to be

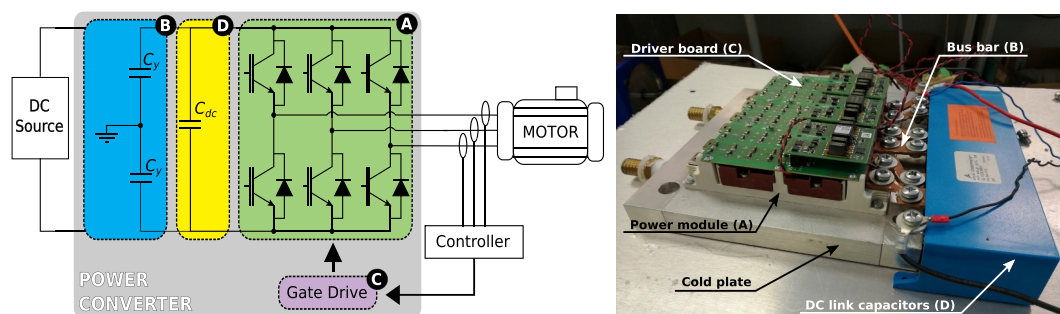


Fig. 6. Typical layout and elements of a three-phase automotive power converter.

**Table 6**  
SiC and GaN material properties compared with Si [134].

Material property	Si	GaN	SiC-4H <sup>(1)</sup>
Band Gap (eV)	1.1	3.4	3.2
Critical field (10 <sup>6</sup> V/cm)	0.25	0.3	2.2
Electron mobility (cm <sup>2</sup> /V-sec)	1350	1000	950
Thermal conductivity (Watts/cm <sup>2</sup> K)	1.5	1.3	3–4

<sup>(1)</sup> The 4H in SiC-4H refers to the crystal structure of the SiC materials.

paired with Si IGBTs [133,140]. However, JBDs have two significant advantages over SBDs. On the one hand, they are able to handle higher voltages and, on the other hand, they exhibit a lower leakage current [148,149]. Typically, blocking voltages of automotive SiC Schottky diodes lay between 600 V and 1700 V, featuring current ranges between 2 A and 47 A (Table 7).

Regarding SiC power transistors, SiC MOSFETs are preferred as active power switches, mainly because they are able to switch at high frequencies, because their gate charge is similar to Si MOSFETs and IGBTs, being normally off, and also because they require relatively simple driver circuits [148,149].

MOSFETs have an intrinsic antiparallel diode (body diode) between the drain terminal and the substrate. For that reason, if necessary, the use of the external freewheeling diode could be discarded, being the body diode which performs this function. There are some modules that follow that criteria. Nevertheless, the use of the external Schottky freewheeling diode is recommended, because the overall efficiency and the reliability is improved, and also because the freewheeling dissipation occurs in a different device from the MOSFETs themselves.

Current automotive SiC MOSFETs have voltage ranges between 400 V and 1700 V, with current capabilities between 2.6 A and 100 A (Table 7). It is expected that commercial products up to 3.3 kV will be available in the near future [148].

Finally, it is important to note that SiC IGBTs are still under development due to reliability problems (mainly due to forward voltage drift). However, some authors consider this technology as the one with the highest potential for future high-voltage applications [139]. Moreover, some manufacturers such as CREE, Infineon, Microsemi and others can make full SiC modules of different topologies (Table 8).

Their commercialization will depend on overcoming reliability problems through the improvement of the quality of the initial semiconductor material [133]. The scientific community is performing significant advances in that field, being relevant examples the converters based on 15 kV/40 A SiC N-IGBT presented in Refs. [150,151], or the series connected 15 kV SiC IGBTs and MOSFETs presented in Ref. [152] for MV power conversion systems.

#### 4.1.2. GaN devices

GaN technology is in its first development stages concerning to power applications. Vertical GaN devices are being considered for research due to their potential. GaN switches are expected to have a 100 times performance improvement over Si-based devices, and a 10 times improvement over SiC, due to the excellent material characteristics such as high electron mobility, high breakdown field and high electron velocity [153]. GaN shows the highest breakdown voltage level with the lowest conduction resistance for the same material area [148]. However, one of the major drawbacks of GaN devices resides in one of their main theoretical advantages, i.e., the ultra-fast switching speeds of these devices (of around 1–2 ns), which makes parasitic inductances become a serious problem [149].

Currently, most of the commercialized GaN Schottky diodes (600 V/10–15 A) are either lateral or quasi-vertical, due to the lack of electrically conducting GaN substrates [133,140]. Moreover, GaN material is very expensive, so that manufacturers prefer to design diodes with heterogenous structures such as silicon, SiC, and even zafire [147]. On

the other hand, the great majority of the existing GaN active switches are High Electron Mobility Transistors (HEMTs) and their derivatives [133,139,140]. An HEMT is a heterojunction device composed by an AlGaN layer formed on top of a GaN substrate. These devices represent a remarkable tradeoff between specific on-resistance and breakdown voltage [133]. GaN HEMTs are inherently normally-on devices, but high power applications require normally-off (safe) devices with high currents and voltage capability [133,153]. One solution for the normally-on challenge is to make a cascode connection of a GaN HEMT with a low voltage Si MOSFET. In that way, the gate drive is the same as for a Si MOSFET (normally-off) [146,149]. However, the main disadvantages or current automotive GaN devices are the low voltage and current ratings (Table 9) and, on the other hand, the need to package two switching devices in a leaded multichip package [146,149]. Additionally, there are only a few GaN power devices available in the market (Table 9), as most of them are prototypes.

#### 4.1.3. Electrical requirements for automotive WBG power stage dimensioning

Once the most suitable power semiconductor devices available in the market have been identified, it is important to define the electrical requirements (in terms of voltage blocking and current handling capabilities) to be met by next generation HEV/EV power converters.

Voltage requirements mainly depend on the nature of the vehicle and electric machine. In this context, nominal voltages ranging from 100 V to 150 V can be typically found in mild HEV battery packs [154]. Regarding heavily electrified vehicles, higher voltages are the norm. For example, nominal voltages between 200 V and 360 V are common in light to medium weight vehicles mounting medium voltage electric machines [44,103,154–156], while voltages close to 800 V–900 V are the norm in heavy duty vehicles including high power voltage machines [156,157]. It is important to note that this voltages can become higher depending on the battery State of Charge (SoC) or during regenerative braking, as well as overvoltages that appear in the switching path due to the parasitic inductances. Depending on the battery pack maximum voltage ratings, SiC or GaN devices belonging to the 600 V, 1200 V or 1700 V families should be selected.

The determination of the current requirements is not straightforward, as it will depend on a number of factors, such as the machine maximum torque and power ratings, and also on its torque per ampere production capabilities [44,158,159]. In synchronous machines based on PMs, field weakening current injection requirements must also be determined considering the worst operation scenario (i.e., considering the minimum dc-link operation voltage) [42,44]. Thus, an analysis of the specific drive would be required for the determination of the exact current requirements. From the available literature, it can be concluded that maximum currents ranging from 200 A to 255 A are common for drive systems including 200 V–400 V battery packs and synchronous machines with power ratings between 50 kW and 70 kW [44,103,160]. Similar requirements can be found for IM technologies, as current ratings of around 235 A are common for 50 kW IMs [47].

Significant current handling capabilities will be required for higher power vehicles or overload operation conditions (80 kW–125 kW). For example, maximum currents between 400 A and 480 A are required for the synchronous machines presented in Refs. [160,161]. For these power ratings, less current would be required in electric drives including high voltage electric machines and battery packs [156]. However, this type of machines/battery packs are, in most cases, intended for higher power applications, requiring significantly higher current ratings.

Thus, considering the actual HEV/EV requirements and automotive SiC and GaN devices in the market, and taking into account the current ratings of discrete devices, converters based on this technology could cover the aforementioned requirements by means of discrete/bare die device parallelization.

The main objective of the parallelization is to increase current

**Table 7**  
Some of automotive grade and automotive oriented SiC discrete devices available on the market.

Company	Device	Packaging	Product name	Voltage (V)	I (A) @ T <sub>c</sub> (°C)			
CREE	MOSFET	TO-247-3	C2M0040120D*	1200	40 @ 100			
			C2M0045170D*	1700	48 @ 100			
			C2M0025120D*	1200	60 @ 100			
			CPM2-1200-0025B	1200	71 @ 100			
			CPM2-1200-0040B	1200	40 @ 100			
	Schottky diode	TO-247-3	CPM2-1700-0045B	1700	48 @ 100			
			C3D20060D*	600	26 @ 135			
			C3D30065D*	650	36 @ 135			
			C5D50065D*	650	50 @ 130			
			C4D40120D*	1200	54 @ 135			
			C4D30120D*	1200	43 @ 135			
			C4D20120A*	1200	25 @ 135			
			CPW5-0650-Z030B	650	30 @ 150			
			CPW5-0650-Z050B	650	50 @ 175			
			CPW5-1200-Z050B	1200	50 @ 175			
			CPW5-1700-Z050B	1700	51 @ 150			
			Global Power	MOSFET	TO-247	GP1T036A060B	1200	50 @ 100
						GP1T025A120B	1200	50 @ 100
						GP1T040A120B	1200	31 @ 100
						GP1T072A060B	600	25 @ 100
GP2D020A120B	1200	24 @ 150						
Schottky diode	TO-247-2L	GP2D020A120B		600	29 @ 150			
		GP2D050A120B		1200	58 @ 150			
		IXYS		MOSFET	SOT-227B	IXFN70N120SK	1200	48 @ 100
						IXFN50N120SK	1200	33 @ 100
						IXFN50N120SiC	1200	35 @ 80
Schottky diode	TO-268AA SOT-227B	MCB60I1200TZ	1200	60 @ 100				
		DCG45X1200NA	1200	40 @ 100				
		DCG85X1200NA	1200	76 @ 100				
		DCG100X1200NA	1200	94 @ 100				
		DCG130X1200NA	1200	114 @ 100				
Microsemi	MOSFET	TO-247	APT40SM120B*	1200	29 @ 100			
			APT70SM70B*	700	41 @ 100			
			APT80SM120B*	1200	55 @ 100			
			APT70SM70J*	700	34 @ 100			
			APT40SM120J*	1200	23 @ 100			
	Schottky diode	TO-247	APT80SM120J*	1200	36 @ 100			
			MSC030SDA120B*	1200	30 @ 140			
			ROHM	MOSFET	Bare Die	S4001	650	70 @ 25
						S4002	650	93 @ 25
						S4003	650	118 @ 25
S2301	1200	40 @ 25						
S4101	1200	55 @ 25						
Schottky diode	TO-247 N	SCT3017AL SCT3022AL	650 650	83 @ 100 65 @ 100				
		SCT3022KL	1200	67 @ 100				
		SCT3030AL	650	49 @ 100				
		SCT3030KL	1200	51 @ 100				
		SCT3040KL	1200	39 @ 100				
		SCH2080KE	1200	28 @ 100				
		SCS215AG*	650	15 @ 175				
		SCS230AE2*, SCS215AE*	650 650	30 @ 130 15 @ 130				
		SCS215AM*	650	15 @ 55				
		SCS215AJ	650	15 @ 120				
		ST Microelectronics	MOSFET	HIP247	SCT50N120	1200	50 @ 100	
					SCT30N120	1200	34 @ 100	
					SCTW100N65G2AG*	650	85 @ 100	
					STPSC40065C-Y *	650	40 @ 130	
					STPSC20H12-Y*	1200	20 @ 150	
Schottky diode	TO-247 TO-220AC/D2PAK TO-247 LL TO-247/TO-220 AB TO-247/TO-220 AC/D2PAK		STPSC40H12C*	1200	40 @ 150			
			STPSC20H065C-Y*	650	20 @ 150			
			STPSC20065-Y*	650	20 @ 140			
			IDW20G120C5	1200	20 @ 150			
			IDW30G120C5B	1200	30 @ 150			
INFINEON	Schottky diode	PG-TO220-2-1 PG-TO247-3	IDW40G120C5B	1200	40 @ 148			
			IDW40G65C5	650	40 @ 110			

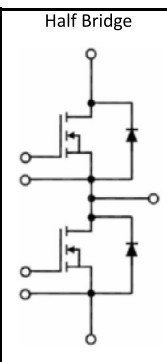
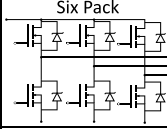
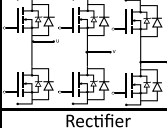
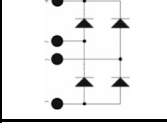
(\*) Product with automotive grade certification.

capability and, therefore, the converter power capability is also increased. The vast majority of manufacturers offer power modules in which each switch is composed of several semiconductors (bare dies) arranged in parallel, to be able to reach the currents required by the application. To achieve this objective, current distribution for each parallelized device must be as equal as possible. However, there are

several factors that cause current imbalances, among others [162]:

- Differences in the internal parameters which characterize each device to be parallelized. On the one hand, these parameters affect the static behaviour. The variation of collector-source saturation voltage ( $V_{DSSat}$ ) and the gate threshold voltage ( $V_{GSth}$ ) with the temperature

**Table 8**  
Some of automotive oriented SiC modules devices available on the market.

	Device	Company	Product name	Voltage (V)	I (A) @ Tc (°C)
	MOSFET module	CREE	CAS120M12BM2	1200	138 @ 90
			CAS300M12BM2	1200	293 @ 90
			CAS300M17BM2	1700	225 @ 90
		Microsemi	APTSM120AM14CD3AG	1200	180 @ 80
			APTMC120AM08CD3AG	1200	190 @ 80
			APTSM120AM09CD3AG	1200	268 @ 80
			APTSM120AM08CT6AG	1200	293 @ 80
			APTMC120AM12CT3AG	1200	165 @ 80
			APTMC120AM09CT3AG	1200	220 @ 80
		ROHM	BSM180D12P2C101	1200	180 @ 60
			BSM120D12P2C005	1200	120 @ 60
			BSM180D12P3C007	1200	180 @ 60
			BSM300D12P2E001	1200	300 @ 60
Semikron	SKM500MB120SC	1200	431 @ 80		
	MOSFET module	CREE	CCS020M12CM2	1200	20 @ 90
	MOSFET module	Microsemi	APTSM120TAM33CTPAG	1200	89 @ 80
			APTMC120TAM17CTPAG	1200	110 @ 80
			APTMC120TAM12CTPAG	1200	165 @ 80
		Semikron	SK45MAHT12SCp	1200	38 @ 70
	Schottky diode module	Global Power	GHXS020A060S-D1	600	25 @ 125
			GHXS030A060S-D1	600	36 @ 150
			GHXS030A120S-D1	1200	30 @ 125
			GHXS045A120S-D1	1200	45 @ 150
		Microsemi	APT40DC60HJ	600	40 @ 100
			APT40DC120HJ	1200	40 @ 100

**Table 9**  
Some of automotive grade and automotive oriented GaN discrete devices available on the market.

Company	Device	Packaging	Product name	Voltage (V)	I (A) @ Tc (°C)
GaN Systems	E-HtMI	GaNPX packaging	GS66516T	650 V	47 @ 100
			GS66516B	650 V	47 @ 100
Transphorm	GaN FET	TO-247	TPH3205WSBQA*	650 V	22 @ 100

(\*) Product with automotive grade certification.

involves a current change. In order to prevent high current imbalances, power transistors must have similar characteristic curves. On the other hand, dynamic behaviour is also affected by the variation of internal parameters with the junction temperature, since devices can present different turn on ( $t_{d,on}$ ) and turn off ( $t_{d,off}$ ) delays which can produce current imbalances [163,164].

- Driver circuit design. An optimal drive circuit gate design is essential, since it has a direct influence over current balance. In this sense, the design must be symmetrical. In order to achieve this objective, driver output impedance must be controlled. There are also in the technical literature various control strategies of common or separate gate [165,166].
- Power circuit layout design. It is fundamental to minimize, as much as possible, parasitic inductances to reduce the voltage peaks caused by  $di/dt$  through the switching path [167].

#### 4.2. Reactive elements and bus bar

As shown in Fig. 6, the power conversion stage may include a number of passive elements between the vehicle battery and the power semiconductors, such as Y-type capacitors ( $C_Y$ ) and dc-link capacitors ( $C_{dc}$ ).

The dc-link capacitor (or dc-link capacitor bank) can be considered

as the most relevant reactive element in an automotive power converter. In order to prevent significant battery degradation, battery current ripple should be kept below 10% of the rated battery current [168,169]. The dc-link capacitor must filter the high frequency current ripple produced by semiconductor switching at the converter input side. On the other hand, as power electronics are one of the major EMI sources in a vehicle, Y capacitors can be mounted from the dc-bus terminals to the vehicle chassis (Fig. 6) for effective EMI reduction [170].

A number of design aspects must be considered when selecting or designing this critical element. Firstly, the capacitor must be rated according to the battery voltage and must be able to withstand the maximum rms current that will circulate through it. The capacitance value must be selected to keep the current ripple below the aforementioned levels. At the same time, the high frequency voltage ripple across the dc-link capacitor should be limited to  $\pm 10\%$  of the rated voltage for all expected load conditions [168,171]. This second aspect is relevant to guarantee a proper torque control [171].

Another critical aspect is the stray inductance (ESL). The capacitor ESL must be low enough to avoid overvoltage failures during semiconductor's turn-off switching and also to reduce switching losses on the semiconductor [169]. This is of particular importance when using WBG semiconductors with high speed switching capabilities (section 4.1).

The dc-link is a bulky element, and one of the main fault sources in modern power converters [172–174], being, in general, its life time shorter than that of the other components of the converter [175]. Thus, proper capacitor dimensioning and thermal managing must be carried out in order to extend the capacitor life cycle [172]. The capacitor parasitic resistance ESR is responsible for its heating; thus, the lower the ESR the better the dc-link reliability.

Aluminium Electrolytic Capacitors (Al-Caps), Metallized Polypropylene Film Capacitors (MPPF-Caps) and high capacitance Multi-Layer Ceramic Capacitors (MLC-Caps) are commonly used in high voltage dc-link applications. In practice, Al-Caps and MLC-Caps allow high energy densities up to  $2\text{ J/cm}^3$  [172]. However, MPPF-Caps are preferred for automotive applications, as they provide a well-balanced performance in terms of cost, ESR value, required capacitance vs current ripple (Fig. 7) and reliability [172,174,176–178]. Fig. 8 shows a performance comparisons between Al-Caps, MPPF-Caps and MLC-Caps. MPPF-Caps have a superior performance, they provide a well-balanced performance for high voltage applications (above 500 V) in terms of ESR and cost. The cost of MPPF-Caps is about 1/3 of Al-Caps, and it implies the possibility to achieve a lower cost, higher power density dc-link design with MPPF-Caps in high ripple current applications, such as in electric vehicles [172].

Table 10 summarizes various automotive grade MPPF dc-link capacitors available on the market, including their most significant features. In general, two packaging technologies can be distinguished:

- Capacitors with integrated bus bars (Fig. 9(a)), which are specifically designed for various particular automotive power module layouts. These solutions provide easy integration and high capacitances with a very low ESL (Table 10).
- Capacitors for PCB or bus bar mounting (Table 10 and Fig. 9(b)). They allow flexible capacitor bank and bus bar designs, which can effectively reduce the value of ESL and improve semiconductors switching dynamics. For example, in Ref. [169], the DC link inductance has been reduced from 15,4 nH to 2,8 nH using an optimized switching cell.

Thus, proper bus bar design with low stray inductance is required when following the PCB or bus bar approach and fast switching WBG devices are used in the power stage [179]. A number of considerations must be taken into account regarding this critical element. On the one hand, power semiconductors and DC-link capacitor geometry must be properly selected in order to optimize the power density, as well as to minimize the bus bar complexity. The bus bar shape will be directly influenced by the power conversion stage required by the specific vehicle drive topology (three-phase, dual three-phase, asymmetric H-bridge, etc.). If capacitor cooling is required, this will also influence the design geometry [180]. On the other, terminal connections have a significant impact on stray inductance and their influence must be considered, and special care must be taken regarding sharp corners and bends, as they can cause eddy currents and, consequently, voltage drops which result in additional losses and heat generation [180]. Finally, it must be borne in mind that the ESR of an MPPF capacitor depends on both capacitor temperature and current ripple frequency. In this case, the temperature dependency is low. However, the ESR significantly increases while increasing the switching frequency of the converter [168]. Thus, this aspect should be carefully analysed in high WBG power converters with high switching frequency operation.

## 5. Advanced power converter thermal management

An effective vehicle cooling system architecture and performance enables a more compact power converter packaging, reducing the propulsion system size and weight, while increasing system reliability and power density [181–184]. Nevertheless, current approaches for power converter cooling, in general, do not simultaneously meet the

future cost, performance and size targets (Table 2). For this reason, thermal management represents one of the major technical challenges for HEV/EV drive designers and manufacturers [181,183].

Thermal resistance ( $R_{th}$ ) is one of the most important parameters to be considered in the design of an automotive power converter. It indicates its heat transfer capability and determines the temperature gradient between the heat source and heatsink. For a layer of a given material, is determined by the material thickness ( $t$ ), thermal conductivity ( $\sigma$ ) and area ( $A$ ). For a multi-layer system, the total is the sum of each layer's [185]:

$$R_{th} = \sum_{i=1}^n \frac{t_i}{\sigma_i A_i}, \quad (4)$$

where  $n$  is the number of layers. For a given steady state power dissipation  $P_D$  (due to semiconductor conduction and switching losses), the junction to coolant  $\Delta T_{j-f}$  temperature gradient in steady state can be obtained as [185]:

$$\Delta T_{j-f} = R_{j-f} P_D, \quad (5)$$

where  $R_{j-f}$  is the total thermal resistance between the semiconductor junction and the coolant. Thus, the aim of an efficient cooling system is to reduce such resistance as much as possible.

Standard air cooling solutions have a relatively high and are heavy and voluminous for automotive purposes so, in general, liquid cooling is preferred [186]. The usage of a cooling loop with the cooling liquid at  $65\text{ }^\circ\text{C}$  was the norm in previous generation electric vehicles. However, current technological trend in HEV cooling architectures consists on using the ICE liquid cooling loop (commonly 50% water, 50% ethylenglicol) to cool both the ICE and the power converter. In this particular scenario, the nominal coolant temperature is of around  $105\text{ }^\circ\text{C}$  [184,187]. Additionally, advanced air cooling solutions using the air flow produced by vehicle motion are also being considered for future EVs and HEVs [181,182,187,188]. These trends imply a high heatsink temperature, so the subsequent cooling systems design must be greatly optimized in order to ensure system reliability.

Cooling technologies are responsible for keeping the operation junction temperatures ( $T_{j,op}$ ) of power semiconductors (Fig. 10) bellow their maximum ratings, preventing device failures. Maximum junction temperatures of  $150\text{ }^\circ\text{C}$  are the norm in current Si Trench 4 IGBTs [189], while higher operation temperature withstanding capabilities can be found in current SiC and GaN technologies (above  $200\text{ }^\circ\text{C}$ ) [181,190–192]. This makes WBG technology attractive for its application in air cooled and high temperature liquid cooled architectures [1,132,181,190]. However, in practice, maximum operation temperatures are limited to  $175\text{ }^\circ\text{C}$  due to the available packaging technologies,

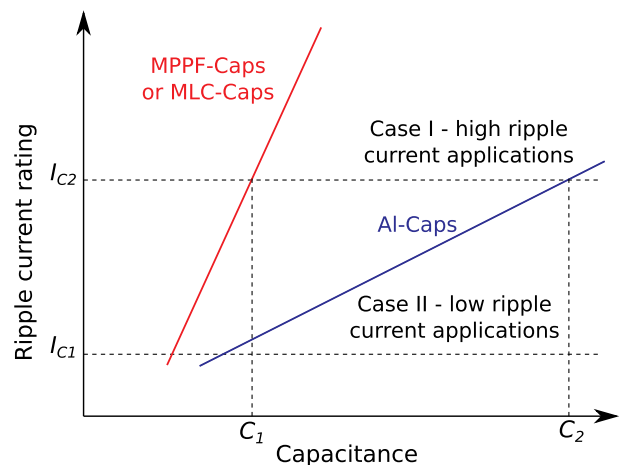


Fig. 7. Capacitance requirements of various capacitor technologies under high current ripple operation (adapted from Ref. [172]).

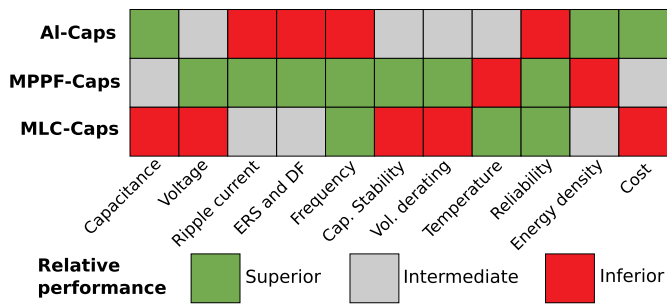


Fig. 8. Performance comparison of the main types of capacitors for dec-link applications (adapted from Ref. [172]).

passive and peripheral components and solder materials [181].

According to a study conducted in Ref. [193] for Si IGBTs and diodes, around 60% of power semiconductor breakages are produced by thermal stress. When power semiconductors experience an overall operation temperature increase of 10 °C, it has been verified that the failure-rate is doubled [194]. The thermal cycle (difference between maximum and minimum temperature of the semiconductors during a whole vehicle driving cycle) can be extremely high. As a variety of materials with diverse expansion coefficients (copper, silicon, plastic materials, etc.), this thermal cycles produces a mechanical stress between the aforementioned materials, producing long term failures in power converters. In this sense, innovative packaging solutions that improve power semiconductor reliability under extreme thermal cycles, such as the solderless SKIM technology, can be found in the industry [189,195].

In the following, this work will focus on the state of the art of current and promising cooling technologies that would facilitate the achievement of the required targets for future vehicle propulsion systems. An in-deep review of each technology, features and challenges will be presented.

### 5.1. Power converter cooling technologies present in the automotive market

#### 5.1.1. Classification of liquid cooling architectures

Liquid cooling is the most widespread cooling technology for automotive applications [188,196]. It is more expensive and complex than air cooling, but it is significantly more efficient [184,185,196–198]. [199] presents a comparison of various air cooling and water cooling methods for power electronics of electric vehicles. In general, liquid cooling can be divided as direct and indirect liquid cooling technologies.

In the indirect cooling approach, there is no direct contact between the power module and the coolant fluid (Fig. 10(a)). In the particular case depicted in Fig. 10(a), the power module is mounted over an aluminium heatsink, including a base plate and separated by an inter-layer of thermal grease. The thermal interface material (TIM) joins thermally the converter baseplate to the heatsink. The TIM has a high thermal resistance [186,196,200], as it accounts between 30% and 50% of the whole thermal resistance [186,201,202]. For this reason, a relatively large temperature gradient between the semiconductor junction and the coolant occurs when dissipating high heat fluxes

Table 10 Automotive grade metallized polypropylene film capacitors available on the market for dc-link applications.

Manufacturer	Family	V <sub>nom</sub> (V)	Capacity (μF)	I <sub>max</sub> (Arms)	ESR (mΩ)	ESL (nH)	Description
Epcos	PCC M651/M652	450	300–500	110–140	0.6	25	For M651/M652 modules
Epcos	PCC HP1	450	300–500	80	0.5–1.0	25–30	For HybridPack 1 packaging
Epcos	PCC HP2	450	500–1000	120–135	0.4–1.0	15	For HybridPack 2 packaging
Kement	C4E series	450	500	120	1.0	15 nH	
Vishay Dale	MKP1849	500	500–1000	120–160	0.25–0.3	15–20	
Vishay Dale	MKP1848	450–1200	1–400	2.5–54.0	1.3–54	>1	For PCB mounting

[203,204]. Many efforts have been focused on the development of advanced TIMs, which reduce their respective R<sub>th</sub> [205–208].

Regarding direct cooling technologies, the power converter thermal resistance is significantly reduced by directly cooling the power module (Fig. 10(b)), as the thermal interface material (TIM) and the base plate are eliminated (R<sub>c-s</sub> case to heatsink thermal resistance is eliminated, Fig. 10(b)). In general, direct cooling technology is preferred for current automotive propulsion systems because of its superior thermal performance [181,184,185,196–198].

Depending on the arrangement of the cold plates, single sided (Fig. 10) or double sided (Fig. 11) cooling architectures can be distinguished. The double-sided structure dissipates heat from both top and bottom sides of the power device (Fig. 11). Therefore, an increase of cooling efficiency is achieved [182,184,186,197,209]. The chips are assembled between two DBC substrates, allowing interconnections within the power devices, resulting in what is often referred to as a sandwich module. As a consequence, new assembly methods without the usage of traditional wire bondings are required, i.e., a solderable front metal can be used to make a planar contact [184,197]. Fig. 11 shows the concept of such planar packaging without wire bondings.

International Rectifier has specifically developed the commercial COOLiR2Die technology for the HEV/EV industry. This technology has been tested in Refs. [197,210]. According to the results obtained, the of the module with dual-sided cooling is 33% lower as compared with single-side cooling.

Denso Corporation, in cooperation with the universities of Cambridge, Nottingham and Oxford, has developed a novel double sided cooled structure, in which the cooling has been carried out using jet-impingement technology [211]. In this design, the of the package can be lower than 0.4 K/W, with less than 40% of the junction to case resistance of a conventional module [211].

The Fraunhofer Institute has developed another similar double sided assembly [212], where the interconnections have been carried out by metal posts between the two DBC substrates. A reduction of 40% (compared with single side cooling) has been achieved using the jet-impingement shower power approach [201].

Alstom/Pearl has developed a similar approach, where the liquid cooling is carried out through finned metal devices joined to one backside [186].

Semikron has developed the SKiN Module, which design combines several cooling technologies. On the one hand, it employs double-sided cooling and, on the other, it eliminates solders and employs the sintering technique for chip-to-substrate junction [212,213]. This allows an increase of about 25% on surge current withstand capability in the power module. Likewise, the between the semiconductor chip and coolant is decreased by up 30%, which results on a power increase or a volume reduction up to 35% [214].

Finally, is also interesting to mention the work presented in Ref. [215], where a reliability design of a dual sided cooled power semiconductor module for EVs/HEVs is carried out. This approach reduces by 50% when compared to a direct liquid cooled module. The base plate is also eliminated achieving a weight and cost saving of about 30%.

Once liquid cooling architectures have been reviewed, cold plate technologies applied in current liquid cooled automotive power converters are presented.



(a) Epcos B25655J4507K005 automotive grade capacitor with integrated bus bar.

(b) Vishay MKP1848 family automotive grade capacitor.

Fig. 9. Automotive grade high power MPPF-Caps.

5.1.2. Cold plate technologies for liquid cooling

Regarding cold plate technologies, the following alternatives can be found in current HEV/EVs: conventional cold plates, microchannel technologies and pin-fin based cold plates.

The performance of conventional cold plates (Fig. 12(a)) is similar to the air cooled heat sinks, using liquid instead of air and taking advantage of higher heat transfer properties of liquids [216]. In Ref. [217], it is demonstrated that, for a three-phase inverter mounting 1.7 kV IGBT technology, the liquid cooling capacity increases from 50 W/cm<sup>2</sup> (for conventional air cooling) to 120 W/cm<sup>2</sup>. This allows increasing converter current density from 40 A/cm<sup>2</sup> to 80 A/cm<sup>2</sup>. The 2004 Toyota Prius also uses a conventional cold plate located in the center of the package to cool the power conversion stage [218].

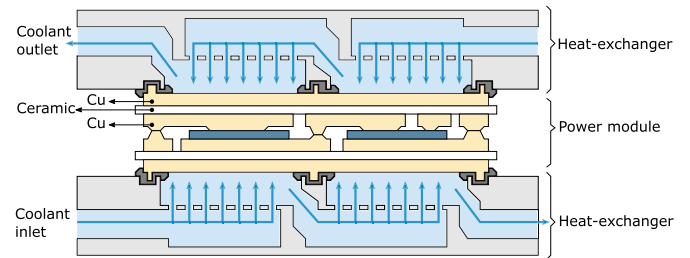
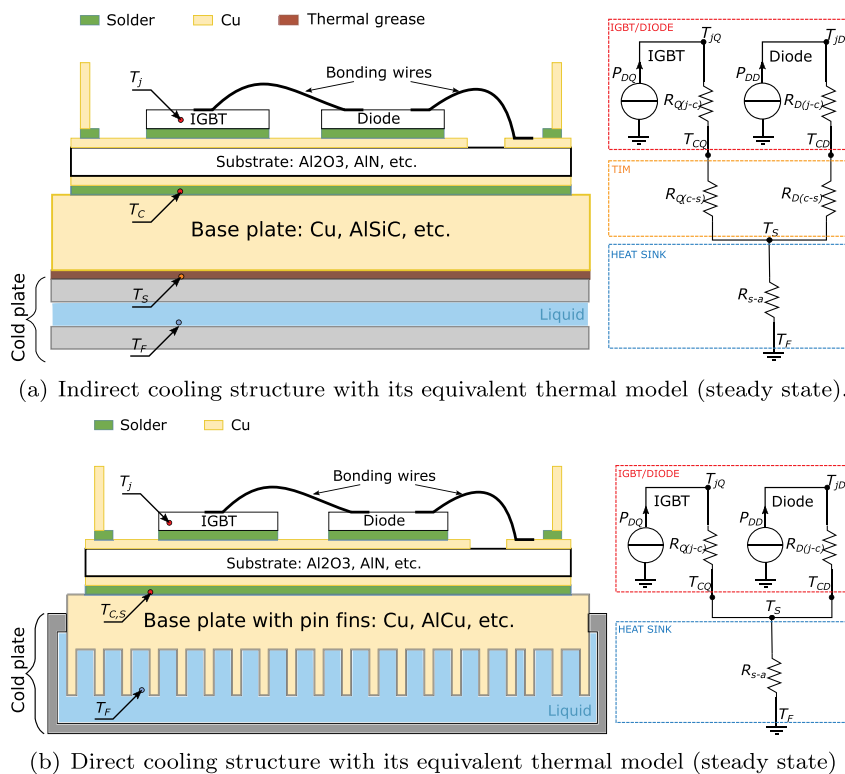


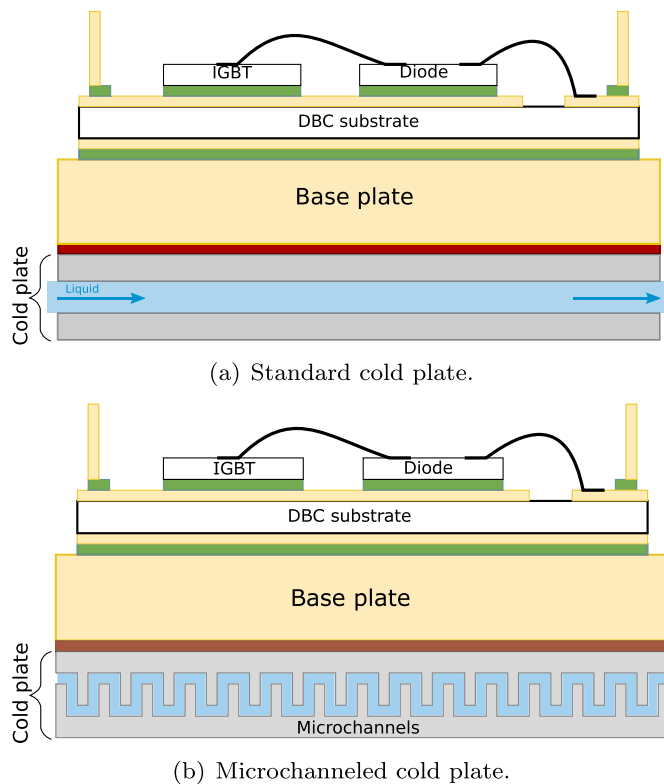
Fig. 11. Double side cooled module [209].



(a) Indirect cooling structure with its equivalent thermal model (steady state).

(b) Direct cooling structure with its equivalent thermal model (steady state)

Fig. 10. Direct and indirect cooling structures (adapted from Ref. [185]). Notes:  $T_j$  = junction temperature,  $T_c$  = case temperature,  $T_s$  = sink temperature,  $T_a$  = ambient temperature,  $P_D$  = total power dissipation,  $R_{j-c}$  = junction to case thermal resistance,  $R_{c-s}$  = case to heat sink thermal resistance,  $R_{s-a}$  = heat sink to ambient thermal resistance.



(a) Standard cold plate.

(b) Microchanneled cold plate.

Fig. 12. Types of cold plates.

Likewise, the automotive grade Infineon HybridPACK 1 (no pin-fin version) [219] requires TIM to mount the module over a base plate.

A great number of cold plate designs have been proposed in the scientific literature, varying the internal structure and material in order to increase its internal surface area and, therefore, improve the heat transfer [182,186,220]. For example, the microchannel cold plate technology has derived from the standard approach, which can be considered as an independent technology and is currently in use in real HEV/EVs, such as the Nissan LEAF.

A microchannel cold plate is formed by using a hole pattern, forming internal channels (Fig. 12(b)). This design provides a large contact surface area and a thin mounting surface, decreasing the value of  $\theta$ . As a result, a heat transfer near  $1000 \text{ W/cm}^2$  can be achieved [216,221]. Other research results are overgoing that value [222]. Although small channels produce higher heat transfers, they also produce more pressure drops, being the latter its mayor drawback [216]. In consequence, many research focuses on pump and micropump technologies in order to overcome this limitation [223–225]. In other researches water has been substituted by eutectic alloys of gallium or indium. The latter is called liquid metal cooling, and it shows promising results beyond the  $1000 \text{ W/cm}^2$  [226–228].

Power modules with pin-fin base plates (Fig. 10) have emerged as an effective and compact solution [229]. This technology consists on a base plate (TIM layer and heat sink are eliminated) with pin fin structure surface, which is immersed into the cooling liquid contained in a trough [230]. A variety of geometries for fins can be found in the literature, which affect the turbulent flow of the coolant. In Refs. [231,232], a comparison of different pin-fin shapes has been done, with regard to the heat transfer coefficient and pressure drop characteristics of each shape. The results show that the staggered arrangement elliptic profile performs better than all other shapes. On the other hand and taking into account a trade off between cooling efficiency and pressure drop, square shape pin-fins have been selected in Ref. [202].

Pin-fin base plates are made from materials with matched thermal expansion coefficients as Aluminium Silicon Composites (AlSiC).

Depending on the proportion of Al, thermal conductivity of the base plate can range from  $160 \text{ W/mK}$  to  $200 \text{ W/mK}$  [233]. New base plate materials, such as AlCu clad materials [229] or aluminium graphite metal-matrix composites (AlC) [234] are under consideration. The latter has a excellent machineability compared to AlSiC [186]. This technology involves simple manufacturing, low pressure drops and large coolant flows. However, the main disadvantage is the temperature gradient obtained when compared to the microchannel technology.

Infineon has developed the automotive grade HybridPACK 1 [219] and HybridPACK 2 [235] IGBT modules based on pin-fin cooling system. Similarly, Fuji Electric has developed pin-fin technology for their automotive grade modules [202].

### 5.1.3. High performance air-cooling in HEV/EVs

Air cooling is not as present as liquid cooling in current HEV/EVs. However, a number of vehicles relying on air cooling technology can be found in the market. For example, Honda Insight HEV (electric power of  $12 \text{ kW}$ ) [236] and Honda Accord drive (launched in 2014) uses this type of cooling technology for power converter cooling [237]. The electric Mini-E also uses an air-cooled AC Propulsion drive system, featuring continuous and peak powers of  $50 \text{ kW}$  and  $150 \text{ kW}$ , respectively [238]. In this scenario, system complexity and cost can be reduced by partially or completely removing the pump, coolant lines, remote heat exchanger, remote heat exchanger fan, and coolant fluid [188]. A study conducted in 2006 estimated a cost saving per vehicle from  $\$150$  to  $\$200$  [239]. Thus, air cooling can be considered as an attractive alternative [181,200]. However, as it is shown in section 5.1.B, the cooling efficiency of such systems is very low, making it difficult to achieve future power density targets.

In order to get the full benefit of the air cooling technology, an optimized system design must carried out. In this context, Tecnia Research and Innovation, in collaboration with Infineon Technologies and GKN EVO eDrive Systems, among others, have developed an in-wheel electric drive (Fig. 13), including a novel thermally and aerodynamically optimized air cooling concept that makes use of the circulating air flow. As a results, a high power density power converter with peak power of  $85 \text{ kW}$  has been achieved [240]. In Ref. [241], The Austrian Institute of Technology, with a number of partners, has developed an integrated drive, featuring smart packaging of power electronics and an integrated air-based thermal management system, reaching experimentally a peak power of  $46 \text{ kW}$  for the power converter.

Taking into account the limitations of air cooling systems, in Refs. [12,37,242,243] it is considered that WBG technologies can potentially facilitate this air cooling solutions without sacrificing drive performance. In this context, Mitsubishi has successfully developed an air cooled SiC inverter of  $150 \text{ kW}$  peak, which has been integrated in a prototype EV [188].



Fig. 13. Air cooled in-wheel drive system developed within the FP7 programme EUNICE project (from Ref. [240]).



## 5.2. Promising thermal solutions for future HEV/EV power stage cooling: two-phase cooling technologies

Two-phase cooling has significant advantages compared to single phase cooling (previously reviewed techniques), such as higher heat transfer rates and efficiency, lower flow rates, isothermal characteristics, lower size and weight, and lower costs [216]. The mayor drawback of this technology is its complexity [216]. Heat transfer is carried out by phase change, i.e., the absorption of thermal energy in the process of evaporation (liquid to vapour) and release of heat in the condensation process (vapour to liquid). A number of two-phase cooling alternatives, such as heat pipes, thermosyphon cooling and thermoelectric cooling can be highlighted [216,244–246].

Heat pipe technology relies on natural forces to transfer heat. Heat pipes are composed by three main elements: container, fluid and wicked structure (Fig. 14). The cooling liquid is evaporated by the heat source at one end of the heat pipe. The vapour is transferred to the opposite end by convection, where it is condensed and the heat is transferred to the environment through a heat exchanger. The vapour cools and condenses into liquid, and is carried back to the heat source through the capillary wick structure along the perimeter of the heat pipe. To form the capillary structure of the heat pipe, a porous material is applied on the inner wall of the pipe. This can be done using either metal foams (such as steel, aluminium, copper or nickel) or using carbon fibres [182,247]. Due to the importance of the wick structure, many works are focused in its development and manufacturing in order to improve the heat transfer [247,248].

The main advantages of heat pipes are their flexibility to be produced in all forms and sizes and the obtained high heat transfer capability (heat fluxes in the range of tens and hundreds of  $\text{W}/\text{cm}^2$ ). Operation temperature limitations and vertical height are their main drawbacks [216,244]. The applicability of this cooling technology in EVs is demonstrated in Refs. [244,249]. However, there are more advanced methods able to increase operation range while improving heat dissipation, as is the case of pulsating heat pipes (PHP) [250–253].

On the other hand, thermosyphon cooling (Fig. 15) is a special type of heat pipe in which the fluid is driven only by gravity forces [216]. The heated liquid is less dense than the cooler water. Therefore, it rises to the top of the cooling system, forcing natural circulation of the cooling liquid. Then, the heat is dissipated to the ambient air through a condenser. Finally, the cold liquid returns to the source and the cooling process starts again. Unlike the heat pipe, it does not incorporate a wick structure through which the condensed working fluid returns. The main disadvantage of this technology is that the system must always be

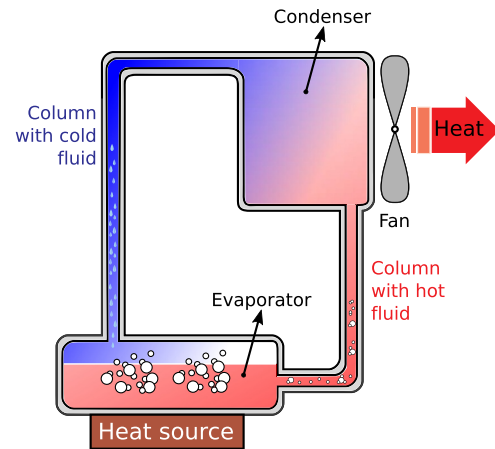


Fig. 15. Thermosyphon cooling operation principle.

positioned in a vertical direction requiring a large amount of space.

Thermosyphon technology achieves heat flux transfer values of around  $230\text{--}240\text{ W}/\text{cm}^2$ , with moderate temperature fluctuations [245]. Many efforts have been done to improve the heat dissipation capability. In Ref. [245], a pump has been inserted in the loop to vary the flow rate of the coolant, allowing a cooling capacity up to  $500\text{ W}/\text{cm}^2$  with a thermal resistance of  $0.125\text{ (Kcm}^2\text{)}/\text{W}$ . Likewise, NREL (National Renewable Energy Laboratory) has developed a thermosyphon based system to cool the power electronics associated to an EV motor. With this approach,  $3.5\text{ kW}$  of semiconductor losses have been dissipated [254]. In Ref. [255], a power module cooling system consisting of a thermosyphon circuit composed by double-sided evaporator has been presented allowing a total dissipation power of  $1500\text{ W}$ .

Thermoelectric cooling (TE) must also be considered. TEs are based on the Peltier effect [256]. When a dc current flows through the module, a heat transference is produced so that each side of the module is cooled or heated respectively (Fig. 16). This allows to cool each semiconductor device individually and uniformly, leading to semiconductor isothermalization [256]. From the electric design point of view, this improves the prediction of device failures, thermal stress, reliability and lifetime of the power module [216,246,249]. Precise temperature control, fast dynamic response, reduced weight and small size are the main advantages of this technology, although the maximum power dissipation is limited to several tens of watts, the efficiency is also low and its cost is high [216,246].

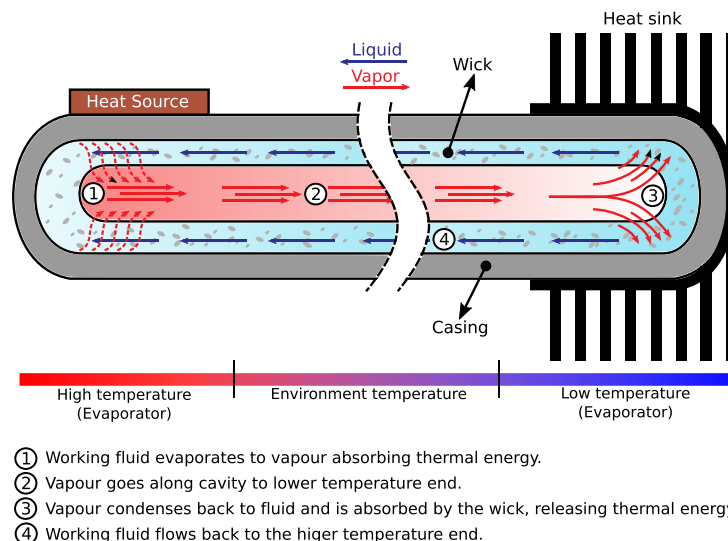


Fig. 14. Heat pipe based cooling operation principle.

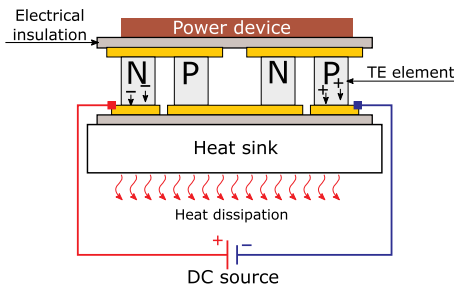


Fig. 16. Diagram of a thermoelectric cooler.

The application of TE cooling to cool power electronics circuits represents a serious handicap [216,246]. However, some recent approaches increase both the efficiency and operation temperature [257]. Hybrid solutions have been also proposed [258], where cold plate liquid cooling is combined with TE cooling. The cold plate is used to cool the power module globally, while the embedded TE is used to ensure the temperature uniformity in the semiconductor.

Finally, the solution presented in Ref. [259] is also worth to mention, as it proposes an innovative two-phase cooling system that uses conventional air conditioning components already available in vehicles, together with a conventional water cooled cold plate, not requiring the development of new technology, while achieving the benefits of two-phase cooling.

### 5.3. Other cooling technologies for high power applications

Spray cooling [260] and jet impingement [261] technologies are somehow popular in the industry. Up to date, they have not been used in marketed HEV/EVs, but they can be considered as promising options, since they are a cooling technologies capable of dissipating the large heat fluxes required in a high-power electronics devices [262]. With spray cooling, very high heat transfer coefficients can be achieved with relatively low coolant flow, leading to light and compact cooling systems [260]. Following this approach, the refrigerant is sprayed into fine droplets that individually impinge on the surface area to be cooled (Fig. 17). Spraying reduces flow rate requirements, but requires a high pressure at the spray nozzle. NREL has developed a cooling system based on spray cooling [203]. This approach can dissipate heat fluxes between 150 and 200 W/cm<sup>2</sup>. Likewise, studies carried out in Refs. [263–266] demonstrate the effectiveness of this cooling approach.

Jet impingement cooling is similar to spray cooling, but is performed with a lower pressure drop at the spray nozzle and a higher coolant flow, reducing noise and the possible spray nozzle clogging [261,267]. As an example [268,269], present a power module cooling system based on this technology. Fig. 18 shows a comparison of heat transfer coefficient shapes of both jet and spray cooling technologies.

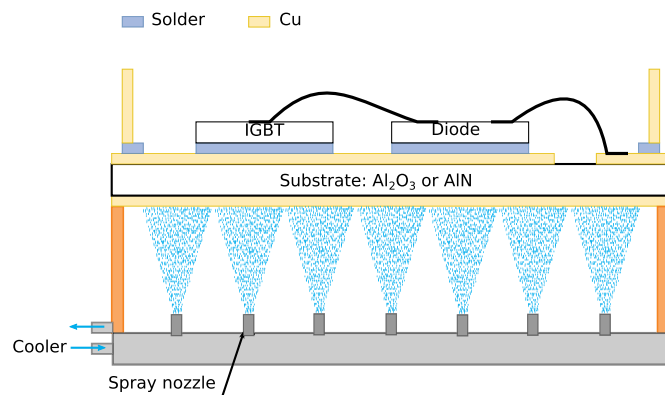


Fig. 17. A power module cooled by spray cooling technology.

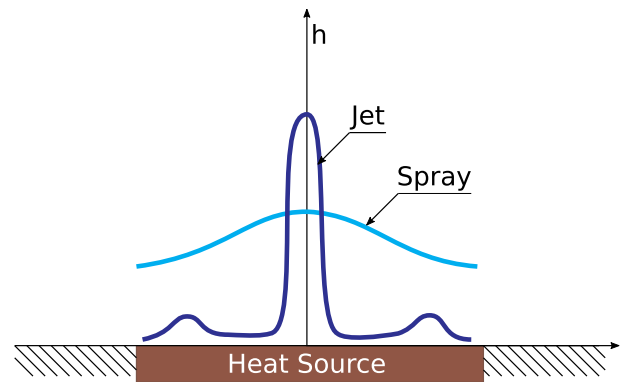


Fig. 18. Heat transfer coefficient shapes of jet impingement and spray cooling.

Danfoss Silicon Power has developed a system called Shower Power which is based on this approach [201]. This eliminates the temperature gradients, allowing to homogeneously cool large power modules, and the parallel placement of many power chips and improving their operation life-cycle [201]. Another advantage of this technology is the possibility of using low-cost materials, such as plastics, to manufacture the cooling device [234]. In Refs. [181,261,267,270], the integration of jet impingement technology in transport applications has been studied with promising results.

## 6. Conclusions

From the reviewed literature, it becomes clear that the development of a sustainable road transport system is of capital importance due to environmental, societal and economical factors. Optimistic forecasts related with future HEV/EV stock evolution should be achieved in order to significantly reduce in road transport GHG emissions. In order to make HEV/EV an attractive option for consumers, a number of technical aspects, such as efficiency, reliability, autonomy and cost must be improved. Being the electric drives a key element of HEV/EV technologies, improvements on the following aspects will be required:

1. A relevant evolution in electric machine technologies will be required for next generation drives. In this context, a significant cost reduction is pursued and, at the same time, power densities must be improved while reducing power losses and improving efficiency.

In some aspects, these targets lead to opposite design concepts. Cost reduction requires the investigation on non rare earth based machine technologies (IMs, SRMs and PM-assisted SynRMs are being mainly considered). However, this technologies have a significantly lower power density than rare earth based machines, making it difficult to achieve the volume reductions targeted by the international agents. Thus, it can be concluded that an extensive research in HSEM technology (with mechanical speeds beyond 10000 rpm) would be conducted in the following years in order to simultaneously achieve the aforementioned targets. Due to the specific requirements of automotive machines, a number of electromechanical aspects and the usage of advanced materials should be investigated for the success of this high speed technology.

2. Torque control of automotive HSEMs can be challenging, mainly due to the high fundamental-to-sampling frequency ratios for proper current regulation, and due to the difficulties to implement reliable field weakening algorithms with such ratios. As it could difficult to implement reliable advanced regulation structures under high nonlinearities (common in automotive machines), it can be concluded that a significant reduction of the execution time of the controller is required for next generation HEV/EV drive controllers.

3. As this controller execution time reduction implies the increase of the switching frequency of the power converter, and taking into account that international agents require a significant improvement in the converter efficiency, it becomes mandatory to introduce WBG technologies with very low switching losses in automotive drive systems power conversion stages. From the available WBG technology, SiC Schottky diodes and SiC MOSFETs could be preferred due to their features. Current handling requirements could be achieved by means of the parallelization of available automotive grade discrete devices, bare dies, or using high power modules from the major WBG power semiconductor manufacturers.

The particularities derived from the high switching speed of such WBG devices will require a proper power converter layout design, specially regarding bus bar and power semiconductor placement. In this context, it is concluded that MPPF-Caps could be preferred due to their well-balance performance for high voltage applications. It will be also required to use capacitors with the lowest ESL possible in order to reduce the stray inductances and, consequently, minimize the over-voltages produced during fast switching.

4. Finally, a number of relevant considerations regarding future HEV/EV drive cooling systems must be taken into account. Being the high power density a mandatory requirement, current state of the art shows that most commercial HEV/EVs use separate liquid-cooling systems for the power electronics and the electric machine. Generally, direct cooling structures are used in the power converters in order to reduce the thermal resistance and improve the reliability of the drive. However, the costs associated with this cooling architecture are high.

One clear tendency for cost reduction leads to the elimination of one of the liquid cooling loops. However, this implies that the nominal coolant temperature of the power semiconductors is increased from 65 °C to 105 °C. This requires an optimization of the cooling system for thermal resistance minimization, and a number of cooling concepts such as double sided cooling or microchanneled cold plates are being implemented and investigated. On the other hand, high performance air-cooling is also being considered to achieve significant cost reductions. However, the cooling efficiency is very low when compared to liquid-cooling, and optimized designs are required in order to make use of the circulating air flow produced when the vehicle is in motion. In both scenarios, reduced power losses of WBG devices would make them mandatory for the power conversion stage.

Last but not least, it is important to point out that a great number of investigations regarding alternative cooling architectures, such as spray cooling, jet impingement cooling, heat pipes, thermosyphon and thermoelectric cooling are being considered, among others. This technologies exhibit interesting features, but they must be further investigated for their implementation in real HEV/EVs.

## Acknowledgements

This work has been partially supported by the Department of Education, Linguistic Policy and Culture of the Basque Government within the fund for research groups of the Basque university system IT978-16, by the Ministerio de Economía y Competitividad of Spain within the project DPI2014-53685-C2-2-R and FEDER funds and by the Government of the Basque Country within the research program ELKARTEK as the project KT4TRANS (KK-2015/00047 and KK-2016/00061), as well as by the program to support the specialization of Ph.D researchers at UPV/EHU ESPDOC16/25.

## References

- [1] Kumar L, Jain S. Electric propulsion system for electric vehicular technology: a

- review. *Renew Sustain Energy Rev* 2014;29:924–40.
- [2] Riba J, Lopez-Torres C, Romeral L, Garcia A. Rare-earth-free propulsion motors for electric vehicles: a technology review. *Renew Sustain Energy Rev* 2016;57:367–79.
- [3] Kumar M, Revankar S. Development scheme and key technology of an electric vehicle: an overview. *Renew Sustain Energy Rev* 2017;70:1266–85. cited By 1.
- [4] Paris declaration on electro-mobility and climate change and call to action. *Tech. rep.* 2015.
- [5] International Energy Agency. Energy technology perspectives 2017. International Energy Agency; June 2017. *Tech. rep.* <https://www.iea.org/etp2017/summary>.
- [6] International Energy Agency. Energy climate change & environment. International Energy Agency; 2016. *Tech. rep.*
- [7] United States Environmental Protection Agency (EPA). Inventory of u.s. greenhouse gas emissions and sinks: 1990-2015. U.S. Government; 2017. *Tech. rep.*
- [8] D. o. E. United Nations, P. D. Social Affairs. World population prospects: the 2017 revision. United Nations; 2018. *Tech. rep.*
- [9] U. Energy Information Administration. Annual energy outlook of 2018. U.S. Energy Information Administration; 2018. *Tech. rep.*
- [10] International Energy Agency. Global EV outlook, beyond on million electric cars. International Energy Agency; 2017. *Tech. rep.*
- [11] Basque energy cluster, Estudio de mercado de vehículo eléctrico y sus infraestructuras de recarga, *Tech. rep.*, Basque energy cluster.
- [12] Rogers S, Boyd S. Overview of the DOE VTO electric drive technologies R&D program. Vehicle Technologies office (U.S Department of Energy); 2016. *Tech. rep.*
- [13] Ko J, Ko S, Son H, Yoo B, Cheon J, Kim H. Development of brake system and regenerative braking cooperative control algorithm for automatic-transmission-based hybrid electric vehicles. *IEEE Trans Veh Technol* 2015;64(2):431–40.
- [14] Xu G, Li W, Xu K, Song Z. An intelligent regenerative braking strategy for electric vehicles. *Energies* 2011;4:1461–77.
- [15] Heydari S, Fajiri P, Rasheduzzaman M, Sabzebar R. Maximizing regenerative braking energy recovery of electric vehicles through dynamic low-speed cutoff point detection. *IEEE Trans Transport Electrification* 2019;5(1):262–70.
- [16] Chen Y, Chen S, Zhao Y, Gao Z, Li C. Optimized handling stability control strategy for a four in-wheel motor independent-drive electric vehicle. *IEEE Access* 2019;7:17017–32.
- [17] Sun H, Wang H, Zhao X. Line braking torque allocation scheme for minimal braking loss of four-wheel-drive electric vehicles. *IEEE Trans Veh Technol* 2019;68(1):180–92.
- [18] Yuan Y, Zhang J, Li Y, Li C. A novel regenerative electrohydraulic brake system: development and hardware-in-loop tests. *IEEE Trans Veh Technol* 2018;67(12):11440–52.
- [19] Miller JF, Howell D. The ev everywhere grand challenge, EVS27 international battery, hybrid and fuel cell electric vehicle symposium. 2013. p. 1–6.
- [20] Horizon 2020. The EU framework programme for research and innovation. <https://ec.europa.eu/programmes/horizon2020>.
- [21] United States Council for automotive research LLC [link]. <http://www.uscar.org/guest/index.php>.
- [22] United nations economical and social commission for Asia and the Pacific. <http://www.unescap.org/>.
- [23] Energy efficiency & renewable energy, multi-year program plan 2011-2015: vehicle technologies program. *Off Energy Eff Renew Energy* 2010. *Tech. rep.*
- [24] Kumar L, Jain S. Electric propulsion system for electric vehicular technology: a review. *Renew Sustain Energy Rev* 2014;29:924–40.
- [25] Chan C. The state of the art of electric, hybrid and fuel cell vehicles. *IEEE*, vol. 95. 2007. p. 704–18.
- [26] Williamson S, Emadi A. Comparative assessment of hybrid electric and fuel cell vehicles based on comprehensive well-to-wheels efficiency analysis. *IEEE Trans Veh Technol* 2005;54(3):856–62.
- [27] Righlot H, Rieck F. Energy chain and efficiency in urban traffic for ice and ev. *Proc. of the EVS conference*. 2013.
- [28] Rousseau A, Ahluwalia R, Deville B, Zhang Q. Well-to-wheels analysis of advanced suv fuel cell vehicles. Society of Automotive Engineers, Inc.; 2003. *Tech. rep.*
- [29] Mahmoudi C, Flah A, Sbita L. An overview of electric vehicle concept and power management strategies. International conference on electrical sciences and technologies in maghreb (CISTEM). 2015. p. 1–6.
- [30] Das H, Tan C, Yatim A. Fuel cell hybrid electric vehicles: a review on power conditioning units and topologies. *Renew Sustain Energy Rev* 2017;76:268–91.
- [31] Conti S, Di Mauro S, Raciti A, Rizzo S, Susinni G, Musumeci S, Tenconi A. Solar electric vehicles: state-of-the-art and perspectives. International annual conference, AETT. 2018. p. 1–6.
- [32] Krishna S, Hari B, Dheerendra S. A comprehensive review on hybrid electric vehicles: architectures and components. *J Mod Transp* 2019;27(2):77–107.
- [33] Enang W, Bannister C. Modelling and control of hybrid electric vehicles (a comprehensive review). *Renew Sustain Energy Rev* 2017;74:1210–39.
- [34] Alagarsamy T, Moulik B. A review on optimal design of hybrid electric vehicles and electric vehicles. International conference for convergence in technology (I2CT). 2018.
- [35] Driving Research and Innovation for Vehicle efficiency and Energy sustainability (USDRIIVE), Electrical and electronics technical team roadmap. *Driving Res Innov Vehicle Eff Energy sustain* 2013. *Tech. rep.*
- [36] Wayne S. High temperature air-cooled power electronics thermal design. National Renewable Energy Laboratory; 2014. *Tech. rep.*
- [37] Ozpineci B. Annual progress report for the electric drive technologies program Oak Ridge National Laboratory; 2016. *Tech. rep.*
- [38] Whaling C. Ev power electronics cost analysis. *IEEE transportation, electrification*

- community newsletter; 2014.
- [39] Gerada D, Mebarki A, Brown N, Gerada C, Cavagnino A, Boglietti A. High-speed electrical machines: technologies, trends, and developments. *IEEE Trans Ind Electron* 2014;61(6):2946–59.
- [40] Bazi A. Electric machines and energy storage technologies in EVs and HEVs for over a century. *Proc. of the international electric machines and drives conference*. 2013. p. 212–9.
- [41] Finken T, Hombitzer M, Hameyer K. Study and comparison of several permanent-magnet excited rotor types regarding their applicability in electric vehicles. *Proc. of the electrical power train conference (emobility)*. 2010.
- [42] Morimoto S, Takeda Y, Hirasa T, Taniguchi K. Expansion of operating limits for permanent magnet motor by current vector control considering inverter capacity. *IEEE Trans Ind Appl* 1990;26(5):866–71.
- [43] Trancho E, Ibarra E, Arias A, Salazar C, López I, Díaz de Guereñu A, Peña A. IPMSM torque control strategies based on LUTs and VCT feedback for robust control under machine parameter variations. *Proc. of the IEEE industrial electronics conference (IECON)*. 2016. p. 2833–8.
- [44] Jung S, Hong J, Nam K. Current minimizing torque control of the IPMSM using ferrari's method. *IEEE Trans Power Electron* 2013;28(12):5603–17.
- [45] Inoue Y, Morimoto S, Sanada M. Control scheme for wide-speed-range operation of synchronous reluctance motor in m-t frame synchronized with stator flux linkage. *IEEJ J Ind Appl* 2013;2(2):98–105.
- [46] Iyer K, Lai C, Mukundan S, Dhulipati H, Mukherjee K, Kar N. Investigation of interior permanent magnet motor with dampers for electric vehicle propulsion and mitigation of saliency effect during integrated charging operation. *IEEE Trans Veh Technol* 2019;68(2):1254–65.
- [47] Boldea I, Tutelea L, Parsa L, Dorrell D. Automotive electric propulsion systems with reduced or no permanent magnet: an overview. *IEEE Trans Ind Electron* 2014;61(10):5696–711.
- [48] Burwell M. Performance cost comparison of induction-motor & permanent-magnet-motor in a hybrid electric car. *Tech Rep* 2013.
- [49] Soderznik M, Rozman K, Kobe S, McGuinness P. The grain-boundary diffusion process in Nd-Fe-B sintered magnets based on the electrophoretic deposition of DyF<sub>3</sub>. *Intermetallics* 2012;23:158–62.
- [50] Thomson M, Chang E, Foto A, Citron-Rivera J, Haddad D, Waldo R, Pinkerton F. Grain-boundary-diffused magnets. the challenges in obtaining reliable and representative bh curves for electromagnetic motor design. *IEEE Electrification Mag* 2017:19–27.
- [51] Jahns T. Getting rare-earth magnets out of ev traction machines. *IEEE Electrification Mag* 2017:6–18.
- [52] Guan Y, Zhu Z, Afinowi I, Mipo J, Farah P. Difference in maximum torque-speed characteristics of induction machine between motor and generator operation modes for electric vehicle application. *Electr Power Syst Res* 2016;136:406–14.
- [53] Sira-Ramirez H, Gonzalez-Montañez F, Cortes-Romero J, Luviano-Juarez A. A robust linear field-oriented voltage control for the induction motor: experimental results. *IEEE Trans Ind Electron* 2013;60(8):3025–33.
- [54] Bozhko S, Dymko S, Kovbasa S, Peresada S. Maximum torque-per-amp control for traction im drives: theory and experimental results. *IEEE Trans Ind Appl* 2017;53(1):181–93.
- [55] Chau K, Li W. Overview of electric machines for electric and hybrid vehicles. *Int J Veh Des* 2014;64(1):46–71.
- [56] Chinmaya K, Singh G. Integrated onboard single-stage battery charger for PEVs incorporating asymmetrical six-phase induction machine. *IET Electr Syst Transp* 2019;9(1):8–15.
- [57] Morimoto S, Ooi S, Inoue Y, Sanada M. Experimental evaluation of a rare-earth-free PMASynRM with ferrite magnets for automotive applications. *IEEE Trans Ind Electron* 2014;61(10):5749–56.
- [58] Bianchi N, Mahmoud Z. An analytical approach to design the PM in PMAREL motors robust toward the demagnetization. *IEEE Trans Energy Convers* 2016;31(2):800–9.
- [59] Bianchi N, Bolognani S, Carraro E, Castiello M, Fornasiero E. Electric vehicle traction based on synchronous reluctance motors. *IEEE Trans Ind Appl* 2016;52(6):4762–9.
- [60] Reddy P, Grace K, El-Refaie A. Conceptual design of sleeve rotor synchronous reluctance motor for traction applications. *IET Electr Power Appl* 2016;10(5):368–347.
- [61] Trancho E, Ibarra E, Arias A, Kortabarria I, Prieto P, Martinez de Alegria I, Andreu J, Lopez I. Sensorless control strategy for light-duty EVs and efficiency loss evaluation of high frequency injection under standardized urban driving cycles. *Appl Energy* 2018;224:647–58.
- [62] Ding W, Yang S, Hu Y, Li S, Wang T, Yin Z. Design consideration and evaluation of a 12/8 high-torque modular-stator hybrid excitation switched reluctance machine for ev applications. *IEEE Trans Ind Electron* 2017:1–6.
- [63] Afjei E, Toliyat H. A novel multilayer switched reluctance motor. *IEEE Trans Energy Convers* 2002;17(2):217–21.
- [64] Desai P, Krishnamurthy M, Schofield N, Emadi A. Novel switched reluctance machine configuration with higher number of rotor poles than stator poles: concept to implementation. *IEEE Trans Ind Electron* 2010;57(2):649–59.
- [65] Lee C, Krishnan R. New designs of a two-phase e-core switched reluctance machine by optimizing the magnetic structure for a specific application: concept, design, and analysis. *IEEE Trans Ind Appl* 2009;45(5):1804–14.
- [66] Nguyen D, Bahri I, Krebs G, Berthelot E, Marchand C, Ralev I, Burkhart B, De Donker R. Efficiency improvement by the intermittent control for switched reluctance machine in automotive application. *IEEE Trans Ind Appl* 2019. <https://doi.org/10.1109/TIA.2019.2906860>.
- [67] Ooi S, Morimoto S, Sanada M, Inoue Y. Performance evaluation of a high power density pmasynrm with ferrite magnets. *IEEE Trans Ind Appl* 2013;49(3):1308–15.
- [68] Vagati A, Boazzo B, Guglielmi P, Pellegrino G. Ferrite assisted synchronous reluctance machines: a general approach. *Proc Int Conf Electr Mach* 2012:1315–21.
- [69] Wang Y, Ionel D, Jiang M, Stretz S. Establishing the relative merits of synchronous reluctance and pm-assisted technology through systematic design optimization. *IEEE Trans Ind Appl* 2016;52(4):2971–8.
- [70] Bilgin B, Emadi A, Kishanamurthy M. Comprehensive evaluation of the dynamic performance of a 6/10 srm for traction application in phevs. *IEEE Trans Ind Electron* 2013;60(7):2564–75.
- [71] Ahn J. Torque control strategy for high performance sr drive. *J Electrical Eng Technol* 2008;3(4):538–45.
- [72] Cabezuelo D, Andreu J, Kortabarria I, Ibarra E, Garate J. Srm converter topologies for ev application: state of the technology. *Proc. of the international symposium on industrial electronics (ISIE)*. 2017. p. 1–6.
- [73] Suryadevara R, Fernandes BG. Control techniques for torque ripple minimization in switched reluctance motor: an overview. *8th IEEE International Conference on In Industrial and Information Systems (ICIS)*. 2013. p. 24–9.
- [74] Petrus V, Pop A, Martis C, Gyselinck J, Iancu V. Design and comparison of different switched reluctance machine topologies for electric vehicle propulsion. *Proc. of the international conference on electrical machines (ICEM)*. 2010. p. 1–6.
- [75] Abbasian M, Fahimi B, Moallem M. High torque double-stator switched reluctance machine for electric vehicle propulsion. *Vehicle power and propulsion conference (VPPC)*. IEEE; 2010. p. 1–5. 2010.
- [76] Finken T, Felden M, Hameyer K. Comparison and design of different electrical machine types regarding their applicability in hybrid electrical vehicles. *Proc Electr Mach Conf* 2008:1–5.
- [77] Cao W, Mecrow B, Atkinson G, Bennett J, Atkinson D. Overview of electric motor technologies used for more electric aircraft (mea). *IEEE Trans Ind Electron* 2012;59(9):3523–31.
- [78] Zeraoulia M, M., Benbouzid D Diallo. Electric motor drive selection issues for hev propulsion systems: a comparative study. *IEEE Trans Veh Technol* 2006;55(6):1756–64.
- [79] Dorrel D, Knight A, Popescu M, Evans L, Staton D. Comparison of different motor design drives for hybrid electric vehicles. *Proc. of the IEEE ECCE conference*. 2010. 3352–2259.
- [80] Yang Z, Shang F, Brown I, Krishnamurthy M. Comparative study of interior permanent magnet, induction, and switched reluctance motor drives for ev and hev applications. *IEEE Trans Transport Electrification* 2015;1(3):245–54.
- [81] Zheng P, Wu F, Lei Y, Sui Y, Yu B. Investigation of a novel 24-slot/14-pole six-phase fault-tolerant modular permanent-magnet in-wheel motor for electric vehicles. *Energies* 2013;6:4980–5002.
- [82] Wang J, Yuan X, Atallah K. Design optimization of a surface-mounted permanent-magnet motor with concentrated windings for electric vehicle applications. *IEEE Trans Veh Technol* 2013;62(3):1053–64.
- [83] Fodorean D, Idoumghar L, Brevilliers M, Minciunescu P, Irima C. Hybrid differential evolution algorithm employed for the optimum design of a high-speed PMSM used for ev propulsion. *IEEE Trans Ind Electron* 2017;64(12):9824–33.
- [84] Fodorean D. Study of a high-speed motorization with improved performances dedicated for an electric vehicle. *IEEE Trans Magn* 2014;50(2):921–4.
- [85] Oksutepe E. In-wheel switched reluctance motor design for electric vehicles by using a pareto-based multiobjective differential evolution algorithm. *IEEE Trans Veh Technol* 2017;66(6):4706–15.
- [86] Kiyota K, Chiba A. Design of switched reluctance motor competitive to 60-kw ipmsm in third-generation hybrid electric vehicle. *IEEE Trans Ind Appl* 2012;48(6):2303–9.
- [87] Juergens J, Fricasse A, Marengo L, Gragger J, De Gennaro M, Ponick B. Innovative design of an air cooled ferrite permanent magnet assisted synchronous reluctance machine for automotive traction application. *Proc. of the international conference on electrical machines (ICEM)*. 2016. p. 803–10.
- [88] Obata M, Morimoto S, Sanada M, Inoue Y. Performance of pmasynrm with ferrite magnets for ev/hev applications considering productivity. *IEEE Trans Ind Appl* 2014;50(4). 2472–2434.
- [89] Zhao W, Chen D, Lipo T, Kwon B. Performance improvement of ferrite-assisted synchronous reluctance machines using asymmetrical rotor configurations. *IEEE Trans Magn* 2015;51(11):1–4.
- [90] Obata M, Morimoto S, Sanada M, Inoue Y. High-performance pmasynrm with ferrite magnet for ev/hev applications. *Proc. of the european power electronics and applications conference (EPE)*. 2013. p. 1–9.
- [91] Olszewski M. Oak ridge national laboratory annual progress report for the power electronics and electric machinery program. Oak Ridge National Laboratory; 2011. Tech. rep.
- [92] Cai H, Guan B, Xu L. Low-cost ferrite pm-assisted synchronous reluctance machine for electric vehicles. *IEEE Trans Ind Electron* 2014;61(10):5741–8.
- [93] Gerada D, Zu X, Zhang H, Galea M, Gerada C, Pickering S. High torque-density in-wheel electrical machine for an electric bus. *Proc. of the IEEE vehicle power and propulsion systems*. 2016. p. 1–6.
- [94] Barrero F, Duran J. Recent advances in the design, modeling, and control of multiphase machines - Part I. *IEEE Trans Ind Electron* 2016;63(1):449–58.
- [95] Barrero F, Duran J. Recent advances in the design, modeling, and control of multiphase machines - Part II. *IEEE Trans Ind Electron* 2016;63(1):459–68.
- [96] Zheng P, Sui Y, Fu Z, Tang P, Wu F, Wang P. Investigation of a five-phase 20-slot/18-pole pmsm for electric vehicles. *Proc. of the international conference on electrical machines and systems (ICEMS)*. 2014. p. 1168–72.
- [97] Karttunen J, Kallio S, Peltoniemi P, Silventoinen P, Pyrhonen O. Decoupled vector control scheme for dual three-phase permanent magnet synchronous machines. *IEEE Trans Ind Electron* 2013;61(5):2185–96.

- [98] Kallio S, Andriollo M, Tortella A, Karttunen J. Decoupled dq model of double-star interior-permanent-magnet synchronous machines. *IEEE Trans Ind Electron* 2013;60(6):2486–94.
- [99] Hu Y, Zhu Z, Liu K. Current control for dual three-phase permanent magnet synchronous motors accounting for current unbalance and harmonics. *IEEE J Emerg Selected Topics Power Electron* 2014;2(2):272–84.
- [100] Patel V, Wang J, Nugraha D, Vuletic R, Tousein J. Enhanced availability of drivetrain through novel multiphase permanent-magnet machine drive. *IEEE Trans Ind Electron* 2015;63(1):469–80.
- [101] Popa D, Fodorean D. Design and performances evaluation of a high speed induction motor used for the propulsion of an electric vehicle. *proc. of the international symposium on power electronics, electrical drives, automation and control*. 2014. p. 88–93.
- [102] Burres T, Campbell S. Benchmarking EV and HEV power electronics and electric machines. *Proc. of the IEEE transportation electrification conference and expo (ITEC)*. 2013. p. 1–6.
- [103] Trancho E, Ibarra E, Arias A, Kortabarria I, Jurgens J, Marengo L, Fricasse A, Gagger J. PM-assisted synchronous reluctance machine flux weakening control for EV and HEV applications. *IEEE Trans Ind Electron* 2018;65(4):2986–95.
- [104] Liu X, Li Y, Liu Z, Ling T, Luo Z. Analysis and design of a high power density permanent magnet-assisted synchronous reluctance machine with low-cost ferrite magnets for EVs/HEVs. *COMPEL* 2016;35(6):910–24.
- [105] Damiano A, Floris A, Fois G, Marongiu I, Porru M, Serpi A. Design of a high-speed ferrite-based brushless DC machine for electric vehicles. *IEEE Trans Ind Appl* 2017;53(5):4279–87.
- [106] Momen F, Rahman K, Son Y. Electrical propulsion system design of chevrolet volt battery electric vehicle. *IEEE Trans Ind Appl* 2019;55(1):376–84.
- [107] Fodorean D. State of the art of magnetic gears, their design, and characteristics with respect to EV application. *INTECH*. 2016.
- [108] Staton D, Boglietti A, Cavagnino A. Solving the more difficult aspects of electric motor thermal analysis in small and medium size industrial induction motors. *IEEE Trans Energy Convers* 2005;20(3):620–8.
- [109] Rahman M, Zhou P. Analysis of brushless permanent magnet synchronous motors. *IEEE Trans Ind Electron* 1996;43(2):256–67.
- [110] Dubas F, Rahideh A. 2-D analytical PM eddy-current loss calculations in slotless PMSM equipped with surface-inset magnets. *IEEE Trans Magn* 2014;50(3):54–73.
- [111] Mekhiche M, Nichols S, Kirtley J, Young J, Boudreau D, Jodoin R. High-speed, high-power density PMSM drive for fuel cell powered HEV application. *Proc. of the electric machines and drives conference (IEMDC)*. 2001. p. 658–63.
- [112] Urasaki N, Senjyu T, Uezato K. A novel calculation method for iron loss resistance suitable in modelling permanent-magnet synchronous motors. *IEEE Trans Energy Convers* 2003;18(1):41–7.
- [113] Kioskeridis I, Margaris N. Loss minimization in induction motor adjustable-speed-drives. *IEEE Trans Ind Electron* 1996;43(1):226–31.
- [114] Tangudu J, Jahns T, Bohn T. Design, analysis and loss minimization of a fractional-slot concentrated winding IPM machine for traction applications. *Proc. of the energy conversion congress and exposition (ECCE)*. 2011. p. 2236–43.
- [115] Meessen K, Thelin P, Soulard J, Lomonova E. Inductance calculations of permanent-magnet synchronous machines including flux change and self- and cross-saturations. *IEEE Trans Magn* 2008;44(10):2324–31.
- [116] Liu X, Chen H, Zhao J, Belahcen A. Research on the performances and parameters of interior pmsm used for electric vehicles. *IEEE Trans Ind Electron* 2016;63(6):3533–45.
- [117] Cintron-Rivera J, Foster S, Zanardelli W, Strangas E. High performance controllers based on real parameters to account for parameter variations due to iron saturation. *NDIA ground vehicle systems engineering and technology symposium*. 2013. p. 1–11.
- [118] Rahman M, Uddin M. Third harmonic injection based nonlinear control of IPMSM drive for wide speed range operation. *IEEE Trans Ind Appl* 2019;55(3):3174–84.
- [119] Pellegrino G, Bojoi RI, Guglielmi P. Unified direct-flux vector control for AC motor drives. *IEEE Trans Ind Appl* 2011;47(5):2093–102.
- [120] Chen K, Sun Y, Liu B. Interior permanent magnet synchronous motor linear field-weakening control. *IEEE Trans Energy Convers* 2016;31(1):159–64.
- [121] Chinchilla M, Arnaltes S, Burgos J. Control of permanent-magnet generators applied to variable-speed wind energy system connected to the grid. *IEEE Trans Energy Convers* 2006;21(1):130–5.
- [122] Pellegrino G, Armando E, Guglielmi P. Optimal exploitation of the constant power region of ipm drives based on field oriented control. *Proc. of the IEEE industry applications conference*. 2007. p. 1335–40.
- [123] Lara J, Xu J, Chandra A. Effects of rotor position error in the performance of field-oriented-controlled pmsm drives for electric vehicle traction applications. *IEEE Trans Ind Electron* 2016;63(8):4738–51.
- [124] Garcia X, Zigmund B, Terlizzi A, Pavlanin T, Salvatore L. Comparison between foc and dte strategies for permanent magnet synchronous motors. *Adv Electr Electron Eng* 2004;76–81.
- [125] Arias A, Caum J, Griño R. Moving towards the maximum speed in stepping motors by means of enlarging the bandwidth of the current controller. *Mechatronics* 2016;40:51–62.
- [126] Arias A, Ibarra E, Trancho E, Griño R, Kortabarria I, Caum J. Comprehensive high speed automotive SM-PMSM torque control stability analysis including novel control approach. *Int J Electr Power Energy Syst* 2019;109:423–33.
- [127] Sepulchre L, Fadel M, Pietrzak-David M. Improvement of the digital control of a high speed pmsm for vehicle application. *Proc. of the eleventh international conference on ecological vehicles and renewable energies (EVER)*. 2016.
- [128] Novak M, Novak Z. Stability issues of high speed pmsm feedback control systems. *Proc. of the european conference on power electronics and applications*. 2013. p. 1–9.
- [129] Altomare A, Guagnano A, Cupertino F, Naso D. Discrete-time control of high-speed salient machines. *IEEE Trans Ind Appl* 2016;52(1):293–301.
- [130] Guagnano A, Rizzello F, G., Cupertino D. Robust control of high-speed synchronous reluctance machines. *IEEE Trans Ind Appl* 2016;52(5):3990–4000.
- [131] Kim H, Degner M, Guerrero J, Briz F, Lorenz R. Discrete-time current regulator design for ac machine drives. *IEEE Trans Ind Appl* 2010;46(4):1425–35.
- [132] Stefanskiy A, Starzak L, Napieralski A. Silicon carbide power electronics for electric vehicles. *International conference on ecological vehicles and renewable energies (EVER)*. 2015. p. 1–9.
- [133] Millan J, Godignon P, Perpina X, Perez-Tomas A, Rebollo J. A survey of wide bandgap power semiconductor devices. *IEEE Trans Power Electron* 2014;29(5):2155–63.
- [134] Ostling M, Ghandi R, Zetterling CM. SiC power devices ; Present status, applications and future perspective. *Symposium on power semiconductor devices and ICs (ISPSD)*. 2011. p. 10–5.
- [135] Shen Z, Omura I. Power semiconductor devices for hybrid, electric, and fuel cell vehicles. *Proc IEEE* 2007;95(4):778–89.
- [136] Choi U, Blaabjerg F, Munk-Nielsen S, Jorgensen S, Rannestad B. Condition monitoring of igt module for reliability improvement of power converters. *Proc. of the IEEE transportation electrification conference and expo (ITEC)*. 2017. p. 602–7.
- [137] Wang Y, Li Y, Wu Y, Dai X, Jones S, Liu G. High power compact automotive igt module with planar packaging technology. *Proc. of PCIM Asia*. 2017. p. 255–9.
- [138] Reimers J, Dorn-Gomba L, Mak C, Emadi A. Automotive traction inverters: current status and future trends. *IEEE Trans Veh Technol* 2019;68(4):3337–50.
- [139] Mantooth HA, Glover MD, Shepherd P. Wide bandgap technologies and their implications on miniaturizing power electronic systems. *IEEE J Emerg Selected Topics Power Electron* 2014;2(3):374–85.
- [140] Millan J. A review of wbg power semiconductor devices. *Semiconductor conference (CAS)*. 2012. p. 57–66.
- [141] Zhang C, Srdic S, Lukic S, Kang Y, Choi E, Tafti E. A sic-based 100 kw high-power-density (34 kw/l) electric vehicle traction inverter. *IEEE energy conversion congress and exposition (ECCE)*. 2018. p. 3380–885.
- [142] Christmann A. Silicon carbide (SiC) semiconductors for xEV are getting closer to reality. *Proc. of the SAE hybrid symposium*. 2018.
- [143] Abdelrahman A, Erdem Z, Attia Y, Youssef M. Wide bandgap devices in electric vehicle converters: a performance survey. *Can J Electr Comput Eng* 2018;41(1):45–54.
- [144] Amano H, Baines Y, Beam E, Borgia M, Bouchet T, Chalker P, Charles M, Chen K, Chowdhury N, Chu R, De Santi C, De Souza M, Decoutere S, Cioccio L, Eckardt B, Egawa T, Fay P, Freedman J, Guido L, Haberlen O, Haynes G, Heckel T, Hemakumara D, Houston P, Hu J, Hua M, Huang Q, Huang A, Jiang S, Kawai H, Kinzer D, Kuball M, Kumar A, Lee K, Li X, Marcon D, Marz M, McCarthy R, M.G., Meneghini M, Morvan E, Nakajima A, Narayanan E, Oliver S, Palacios T, Piedra D, Plissonnier M, Reddy R, Sun M, Thayne I, Torres A, Trivellin N, Unni V, Ureni M, Van Hove M, Wallis D, Wang J, Xie J, Yagi S, Yang S, Youtsey C, Yu R, Zanoni E, Zeltner S, Zhang Y. The 2018 GaN power electronics roadmap. *J Phys D Appl Phys* 2018;51(16):1–48.
- [145] Microsemi PPG, Gallium nitride (GaN) versus silicon carbide (SiC) in the high frequency (RF) and power switching applications, Tech. rep., Microsemi.
- [146] Shirabe K, Swamy MM, Kang JK, Hisatsune M, Wu Y, Kebort D, Honea J. Efficiency comparison between Si-IGBT-Based drive and GaN-based drive. *IEEE Trans Ind Appl* 2014;50(1):566–72.
- [147] Kaminski N, Hilt O. SiC and GaN devices - wide bandgap is not all the same, *IET Circuits, Devices Syst* 2014;8(3):227–36.
- [148] Huang AQ. Power semiconductor devices for smart grid and renewable energy systems. *Proc IEEE* 2017;105(11):2019–47.
- [149] White RV. GaN: the challenges ahead [white hot]. *IEEE Power Electron Mag* 2014;1(1):54–6.
- [150] Madhusoodhanan S, Mainali K, Tripathi AK, Kadavelugu A, Patel D, Bhattacharya S. Power loss analysis of medium-voltage three-phase converters using 15-kv ;40-a sic n-igt. *IEEE J Emerg Selected Topics Power Electron* 2016;4(3):902–17.
- [151] Kadavelugu A, Bhattacharya S, Ryu S-H, Van Brunt E, Grider D, Agarwal A, Leslie S. Characterization of 15 kv sic n-igt and its application considerations for high power converters. *Energy conversion congress and exposition (ECCE)*. IEEE; 2013. p. 2528–35. 2013.
- [152] Vechalapu K, Negi A, Bhattacharya S. Comparative performance evaluation of series connected 15 kv sic igt devices and 15 kv sic mosfet devices for mv power conversion systems. *IEEE energy conversion congress and exposition*. ECCE; 2016. p. 1–8.
- [153] Boutros K, Chu R, Hughes B. GaN power electronics for automotive application. *IEEE energytech*. 2012. p. 1–4.
- [154] Ye H, Emadi A. Traction inverters in hybrid electric vehicles. *Proc. of the transportation and electrification conference and expo (ITEC)*; 2012. p. 1–6.
- [155] Kerns B, Lindsay T, Williams T, Eberle W. A control algorithm to reduce electric vehicle battery pack rms currents enabling a minimally sized supercapacitor pack. *Proc. of the transportation electrification conference and expo (ITEC)*. 2017. p. 376–80.
- [156] Kim H, Chen H, Zhu J, Maksimovic D, Erickson R. Impact of 1.2kv sic-mosfet ev traction inverter on urban driving. *Proc. of the IEEE workshop on wide bandgap power devices and applications (WiPDA)*. 2016. p. 78–83.
- [157] Huang K, Xiang C, Ma Y, Wang W, Langari R. Mode shift control for a hybrid heavy-duty vehicle with power-split transmission. *Energies* 2017;10(2):1–18.
- [158] Yousefi-Talouki A, Pescetto P, Pellegrino G. Sensorless direct flux vector control of synchronous reluctance motors including standstill, mtpa, and flux weakening.

- IEEE Trans Ind Appl 2017;53(4):3598–608.
- [159] Seo S, Park G, Kim Y, Jung S. Design method on induction motor of electric vehicle for maintaining torque performance at field weakening region. Proc. of the electrical machine and systems (ICEMS). 2017. p. 1–5.
- [160] Nguyen Q, Petrich M, Roth-Stielow J. Implementation of the mtpa and mtpv control with online parameter identification for a high speed ipmsm used as traction drive. Proc. of the international power electronics conference. 2014. p. 318–23.
- [161] Nguyen BH, Do HV, Minh CT. High performance current control of ipmsm for electric vehicles drives using disturbance observer. Proc. of the vehicle power propulsion conference (VPPC). 2015. p. 1–5.
- [162] Matallana A, Andreu J, Kortabarria I, Planas E, de Alegría IM. Estado de la tecnología de los dispositivos sic y gan. Seminario Anual de Automtica, Electronica Industrial e Instrumentacin (SAAEI). 2016. p. 1–6.
- [163] Wang X, Zhao Z, Yuan L. Current sharing of IGBT modules in parallel with thermal imbalance. IEEE energy conversion congress and exposition. 2010. p. 2101–8.
- [164] Lator R. Static and dynamic behavior of paralleled igbts. IEEE Trans Ind Appl 1992;28(2):395–402.
- [165] A. Wintrich, U. Nicolai, W. Tursky, T. Reimann, Application manual power semiconductor, SEMIKRON International GmbH.
- [166] Volke A, Hornkamp M. IGBT modules. Technologies, driver and application. Infineon Technologies AG; 2017.
- [167] Chen N, Chimento F, Nawaz M, Wang L. Dynamic characterization of parallel-connected high-power IGBT modules. IEEE Trans Ind Appl 2015;51(1):539–46.
- [168] Wen H, Xiao W, Wen X, Armstrong P. Analysis and evaluation of dc-link capacitors for high-power-density electric vehicle drive systems. IEEE Trans Veh Technol 2012;61(7):2950–64.
- [169] Neeb C, Teichrib J, De Donker R, Boettcher L, Ostmann A. A 50 kw igbt power module for automotive applications with extremely low dc-link inductance. Proc. of the european power electronics and applications conference (EPE-ECCE). 2014. p. 1–10.
- [170] Gao X, Su D. Suppression of a certain vehicle electrical field and magnetic field radiation resonance point. Proc. of the vehicle and power propulsion conference (VPPC), vol. 67. 2018. p. 226–34.
- [171] Aten M, Towers G, Whitley C, Wheeler P, Clare J, Bradley K. Reliability comparison of matrix and other converter topologies. IEEE Trans Aerosp Electron Syst 2006;42(3):867–75.
- [172] Wang H, Blaabjerg F. Reliability of capacitors for dc-link applications in power electronic converters-an overview. IEEE Trans Ind Appl 2014;50(5):3569–78.
- [173] Kolar J, Round S. Analytical calculation of the rms current stress on the dc-link capacitor of voltage-pwm converter systems. IEE Proc Electr Power Appl 2006;153(4):535–43.
- [174] Wechsler A, Mecrow B, Atkinson D, Bennett J, Benarous M. Condition monitoring of dc-link capacitors in aerospace drives. IEEE Trans Ind Appl 2012;48(6):1866–74.
- [175] Pu X, Nguyen T, Lee D, Lee K, Kim J. Fault diagnosis of dc-link capacitors in three-phase ac/dc pwm converters by online estimation of equivalent series resistance. IEEE Trans Ind Electron 2013;60(9):4118–27.
- [176] Winterborne D, Ma M, Wu H, Pickert V, Widmer J, Barrass P, Shah L. Capacitors for high temperature dc link applications in automotive traction drives: current technology and limitations. Proc. of the european conference on power electronics and applications (EPE). 2013. p. 1–7.
- [177] Brubaker M, Hosking T, Von Kampen T. Life testing of high-value annular form factor DC link capacitors for applications with 105 C coolant. Proc. of the power electronics and intelligent motion conference (PCIM). 2011. p. 1–9.
- [178] Ohtsuka H, Anraku F. Development of inverter for 2006 model year civic hybrid. Proc. of the power conversion conference (PCC). 2007. p. 1596–600.
- [179] Stewart J, Neely J, Delhotal J, Flicker J. Dc link bus design for high frequency, high temperature converters. Proc. of the applied power electronics conference and exposition (APEC). 2017. p. 809–15.
- [180] Dorneles A, Guo J, Eull M, Danen B, Gibson J, Bilgin B, Emadi A. Bus bar design for high-power inverters. IEEE Trans Power Electron 2017;33(3):2354–67.
- [181] Kelly k, Abraham T, Bennion K, Bharathan D, Narumachi S, O'keefe M. Assessment of thermal control technologies for cooling electric vehicle power electronics. Electric vehicle symposium (EVS). 2007. p. 1–6.
- [182] Kang S, Aavid T. Advanced cooling for power electronics. Conference on integrated power electronics systems (CIPS). 2012. p. 1–8.
- [183] Kang S, et al. all, Cooling for EV and HEV applications. Applied Power electronics conference (APEC). 2014. p. 1–6.
- [184] Wang Y, Dai X, Liu G, Li D, Jones S. An overview of advanced power semiconductor packaging for automotive system. Conference on integrated power electronics systems (CIPS). 2016. p. 1–6.
- [185] Wang Y, Jones S, Dai A, Liu G. Reliability enhancement by integrated liquid cooling in power igbt modules for hybrid and electric vehicles. Microelectron Reliab 2014;54(9):1911–5.
- [186] Schulz-Harder J. Review of highly integrated solutions for power electronic devices. Conference on Integrated power systems (CIPS). 2008. p. 1–7.
- [187] Power Electronics FreedomCAR, Machines Electrical. Electrical and electronics technical team roadmap. FreedomCAR Power Electron Electr Mach 2013. Tech. rep.
- [188] Wayne S. High temperature air-cooled power electronics thermal design. National Renewable Energy Laboratory; 2016. Tech. rep.
- [189] Wintrich A, Nicolai U, Tursky W, Reinmann T. Power semiconductors application manual. second ed. Semikron International GmbH; 2015.
- [190] Ozzipinci B. Oak ridge national laboratory annual progress report for the electric drive technologies program. Tech. rep. Oak Ridge National Laboratory, Electrical and Electronics Systems Research Division; 2016.
- [191] Brokaw W, Elmes J, Grummel B, Shen ZJ, Wu TX. Silicon carbide high-temperature packaging module fabrication. IEEE workshop on wide bandgap power devices and applications. 2013. p. 178–81.
- [192] Lamichhane RR, Ericsson N, Frank S, Britton C, Marlino L, Mantooth A, Francis M, Shepherd P, Glover M, Perez S, McNutt T, Whitaker B, Cole Z. A wide bandgap silicon carbide (sic) gate driver for high-temperature and high-voltage applications. International symposium on power semiconductor devices IC's (ISPSD). 2014. p. 414–7.
- [193] Ciappa M, Carbonanni F. Lifetime prediction and design of reliability tests for high power devices in automotive applications. IEEE Trans Device Mater Reliab 2003;3:191–6.
- [194] Du B, Hudgins JL, Santi E, Bryant AT, Palmer PR, Mantooth HA. Transient electrothermal simulation of power semiconductor devices. IEEE Trans Power Electron 2010;25(1):237–48.
- [195] Stockmeier T. From packaging to un-packaging trends in power semiconductor modules. International symposium on power semiconductor devices and ICs. 2008. p. 12–6.
- [196] Wang Y, Dai X, Liu G, Wu Y, Li D, Jones S. Integrated liquid cooling automotive igbt module for high temperatures coolant application. International exhibition and conference for power electronics, intelligent motion. Renewable Energy and Energy Management (PCIM); 2015. p. 1–7.
- [197] Marcinkowski J. Dual-sided cooling of power semiconductor modules. International exhibition and conference for power electronics, intelligent motion. Renewable Energy and Energy Management (PCIM); 2014. p. 1–7.
- [198] Higuichi K, Kitamura A, Arai H, Ichimura T, Gohara H, Dietrich P, Nishiura A. An intelligent power module with high accuracy control system and direct liquid cooling for hybrid system. Power electronics — intelligent motion — renewable energy — energy management (PCIM). 2014. p. 1–8.
- [199] Nonneman J, TJollyn I, Clarie N, Weckx S, Sergeant P, Paepe MD. Model-based comparison of thermo-hydraulic performance of various cooling methods for power electronics of electric vehicles. 2018.
- [200] O'keefe M, Bennion K. Comparison of hybrid electric vehicle power electronics cooling options. Vehicle power and propulsion conference. 2007. p. 1–6.
- [201] Danfoss Silicon Power, Showerpower cooling concept, Tech. rep., Danfoss Silicon Power.
- [202] Hitachi T, Gohara H, Naganue F. Direct liquid cooling igbt module for automotive applications. Fuji Electr Rev 2012;57:55–9.
- [203] Mudawar I, Bharathan D, Kelly K, Narumanchi S. Two-phase spray cooling of hybrid vehicle electronics. IEEE Trans Compon Packag Technol 2009;32(2):501–12.
- [204] Krishnamurthy M. Electric vehicle power electronics., ED&EC Kaboratory; 2014. Tech. rep.
- [205] National Renewable Energy Laboratory (NREL). Advanced thermal interface materials (TIMs) for power electronics, tech. Rep. National Renewable Energy Laboratory; 2009.
- [206] Nguyen M, Brandi J. Development of an advanced thermal interface material for high power devices. IEEE semiconductor thermal measurement and management symposium. 2011. p. 333–6.
- [207] Chen S, Lee N-C. High performance thermal interface materials with enhanced reliability. IEEE semiconductor thermal measurement and management symposium (SEMI-THERM). 2012. p. 348–53.
- [208] Pan CA, Yeh CT, Qiu WC, Lin RZ, Hung LY, Ng KT, Lin CF, Chung CK, Jiang DS, Hsiao CS. Assembly and reliability challenges for next generation high thermal tim materials. Electronic components and technology conference (ECTC). 2017. p. 2033–9.
- [209] Skuriat R. Direct jet impingement cooling of power electronics PhD. thesis University of Nottingham; June 2012.
- [210] Marcinkowski J. Innovative coolir<sup>2TM</sup> packaging platform with dual-side cooling advances hev and evs progress. Int Rectifier 2013. Tech. rep.
- [211] Buttay C, Rashid J, Johnson CM, Ireland P, Udrea F, Amaratunga G, Malhan RK. High performance cooling system for automotive inverters. Conference on power electronics and applications. 2007. p. 1–9.
- [212] Schneider-Ramelow M, Baumann T, Hoene E. Design and assembly of power semiconductors with double-sided water cooling. 5th international conference on integrated power electronics systems. 2008. p. 1–7.
- [213] Gobl C, Faltenbacher J. Low temperature sinter technology die attachment for power electronic applications. International conference on integrated power electronics systems (CIPS). 2010. p. 1–7.
- [214] Scheuermann U. Reliability of planar skin interconnect technology (invited). Proc. of the international conference on integrated power electronics systems (CIPS). 2012. p. 1–8.
- [215] Wang Y, Li Y, Liu X, Li H, Dai X, Wu Y, Liu G. Reliability design of dual sided cooled power semiconductor module for hybrid and electric vehicles. International conference on integrated power electronics systems. 2018. p. 1–4.
- [216] Laloya E, Lucía O, Sarnago H, Burdío JM. Heat management in power converters: fro, state of the art to future ultrahigh efficiency systems. IEEE Trans Power Electron 2016;31(11):7896–908.
- [217] Meysenc L, Jylhakallio M, Barbosa P. Power electronics cooling effectiveness versus thermal inertia. IEEE Trans Power Electron 2005;20(3):687–93.
- [218] Olszewski M. Evaluation of 2004 toyota prius hybrid electric drive system. Oak Ridge National Laboratory; 2005. Tech. rep.
- [219] Infineon. Evaluation kit for applications with hybridpack<sup>TM</sup>1 module. Infineon 2012. Tech. rep.
- [220] Blinov A, Vinnikov D, Lehtla T. Cooling methods for high-power electronic systems. Sci J Riga Tech Univ Power Electr Eng 2011;29(1):79–86.

- [221] Faulkner D, Khotan M, Shekarriz R. Practical design of a 1000 w/cm<sup>2</sup> cooling system [high power electronics. Annual IEEE semiconductor thermal measurement and management symposium. 2003. p. 223–30.
- [222] Jung KW, Kharangate CR, Lee H, Palko J, Zhou F, Asheghi M, Dede EM, Goodson KE. Microchannel cooling strategies for high heat flux (1 kw/cm<sup>2</sup>) power electronic applications. IEEE intersociety conference on thermal and thermomechanical phenomena in electronic systems (ITherm). 2017. p. 98–104.
- [223] Jiang Linan, Mikkelsen J, Koo Jae-Mo, Huber D, Yao Shuhuai, Zhang Lian, Zhou Peng, Maveety JG, Prasher R, Santiago JG, Kenny TW, Goodson KE. Closed-loop electroosmotic microchannel cooling system for VLSI circuits. IEEE Trans Compon Packag Technol 2002;25(3):347–55.
- [224] Duan B, Guo T, Luo M, Luo X. A mechanical micropump for electronic cooling. Intersociety conference on thermal and thermomechanical phenomena in electronic systems (ITherm). 2014. p. 1038–42.
- [225] Youcef B, Yvan A. Power electronics cooling of 100 w/cm<sup>2</sup> using ac electroosmotic pump. IEEE Trans Power Electron 2014;29(1):449–54.
- [226] Zhang R, Hodes M, Lower N, Wilcoxon R. Thermo-fluid characteristics of a minichannel heat sink cooled with liquid metal. IEEE semiconductor thermal measurement and management symposium. 2013. p. 159–65.
- [227] Zhang R, Hodes M, Lower N, Wilcoxon R. Water-based microchannel and galinstan-based minichannel cooling beyond 1 kw/cm<sup>2</sup> heat flux. IEEE Trans Compon Packag Manuf Technol 2015;5(6):762–70.
- [228] Liu N, Jin Y, Miao M, Cui X. Optimization of heat transfer of microchannels in Itc substrate with via holes and liquid metal. Conference on electronic packaging technology (ICEPT). 2016. p. 1135–9.
- [229] Uhlemann A. Investigation on alcu-clad base plates and a new by-pass cooler for pin fin power modules. Conference on integrated power electronics systems (CIPS). 2014. p. 1–4.
- [230] Liang Z, Li L. Hybridpack2 advanced cooling concept and package technology for hybrid electric vehicles. Vehicle power and propulsion conference. 2008. p. 1–5.
- [231] Sahiti N, Lemouedda A, Stojkovic D, Durst F, Franz E. Performance comparison of pin fin in-duct flow arrays with various pin cross-sections. Appl Therm Eng 2006;26(11):1176–92.
- [232] Hasan MI, Tbena HL. Enhancing the cooling performance of micro pin fin heat sink by using the phase change materials with different configurations. International conference on advance of sustainable engineering and its application (ICASEA). 2018. p. 205–9.
- [233] Moores KA, Joshi YK, Schiroky GH. Thermal characterization of a liquid cooled alsic base plate with integral pin fins. IEEE Trans Compon Packag Technol 2001;24(1):213–9.
- [234] Schulz-Harder J. Efficient cooling of power electronics. International conference on power electronics systems and applications. 2009. p. 1–4.
- [235] Infineon. Hybridpack<sup>TM</sup> 2 power module for hybrid- and electric vehicles. Infineon 2012. Tech. rep.
- [236] .
- [237] Staunton R, Burrett T, Marlino L. Evaluation of 2005 honda accord hybrid electric drive system. Tech. rep. Oak Ridge National Laboratory; 2006.
- [238] AC Propulsion partners with BMW to build 500 electric vehicles. AC Propulsion; 2008. Tech. rep.
- [239] Hsu J, Staunton R, Starke M. Barriers to the application of high-temperature coolants in hybrid electric vehicles. Oak Ridge National Laboratory; 2006. Tech. rep. Technical Report ORNL/TM-2006/514.
- [240] Peña A. Final report summary - eunice (eco-design and validation of in-wheel concept for electric vehicles). Tech. rep. 2015.
- [241] De Gennaro M. Synemo report summary Austrian Institute of Technology; 2016. Tech. rep. [http://cordis.europa.eu/result/rcn/192394/\\$\\_\\$.en.html](http://cordis.europa.eu/result/rcn/192394/$_$.en.html).
- [242] Chinthavali M, Cristopher J, Arimilli R. Feasibility study of a 55-kw air-cooled automotive inverter. Proc. of the IEEE applied power electronics conference (APEC). 2012. p. 2246–53.
- [243] Wrzeczonko B, Bortis D, Kolar J, A. 120c ambient temperature forced air-cooled normally-off sic jfet automotive inverter system. IEEE Trans Power Electron 2014;29(5):2345–58.
- [244] Hirasawa T, Ikeda M, Sasaki C. Thermal management system with heatpipe for in vehicle electric devices vol. 44. 2013. p. 20–5.
- [245] Battaglia F, Singer F, Dessiatoun SV, Ohadi MM. Comparison of near source two-phase flow cooling of power electronics in thermosiphon and forced convection modes. IEEE intersociety conference on thermal and thermomechanical phenomena in electronic systems (ITherm). 2017. p. 752–8.
- [246] Li C, Jiao D, Jia J, Guo F, Wang J. Thermoelectric cooling for power electronics circuits: modeling and active temperature control. IEEE Trans Ind Appl 2014;50(6):3995–4005.
- [247] Nishikawara M, Nagano H. Optimization of wick shape in a loop heat pipe for high heat transfer. Int J Heat Mass Transf 2017;104(Supplement C):1083–9.
- [248] Vasiliev L, Lossouarn D, Romestant C, Alexandre A, Bertin Y, Piatsiushyk Y, Romanenkov V. Loop heat pipe for cooling of high-power electronic components. Int J Heat Mass Transf 2009;52(1):301–8.
- [249] Brito FP, Martins J, Goncalves LM, Sousa R. Modelling of thermoelectric generator with heat pipe assist for range extender application. Annual conference of the IEEE industrial electronics society (IECON). 2011. p. 4589–95.
- [250] Mamelì M, Marengo M, Zinna S. Thermal simulation of a pulsating heat pipe: effects of different liquid properties on a simple geometry. Heat Transf Eng 2012;33(14):1177–87.
- [251] Burban G, Ayel V, Alexandre A, Lagonotte P, Bertin Y, Romestant C. Experimental investigation of a pulsating heat pipe for hybrid vehicle applications. Appl Therm Eng 2013;50(1):94–103.
- [252] de Vries S, Florea D, Homburg F, Frijns A. Design and operation of a tesla-type valve for pulsating heat pipes. Int J Heat Mass Transf 2017;105(Supplement C):1–11.
- [253] X. H. Z. P. Y. L. X. D. M. W. W. L. Thermal characteristic and analysis of micro-channel structure flat plate pulsating heat pipe with silver nanofluid. IEEE Access 2019;7:51724–34.
- [254] Narumanchi S, Moreno G, Jeffers J. A passive two-phase cooling system for automotive power electronics. Annual IEEE semiconductor thermal measurement and management symposium. 2014. p. 1–6.
- [255] Agostini F, Gradinger T, de Falco C. Simulation aided design of a two-phase thermosiphon for power electronics cooling. Annual conference of the IEEE industrial electronics society (IECON). 2011. p. 1560–5.
- [256] Mole CJ, Foster DV, Feranchak RA. Thermoelectric cooling technology. IEEE Trans Ind Appl IA- 1972;8(2):108–25.
- [257] Strickland E. A new kind of cool. IEEE Spectrum 2011;48(6). 16–16.
- [258] Wang P, McCluskey P, Bar-Cohen A. Hybrid solid- and liquid-cooling solution for isothermalization of insulated gate bipolar transistor power electronic devices. IEEE Trans Compon Packag Manuf Technol 2013;3(4):601–11.
- [259] Aranzabal I, Martínez de Alegría I, Delmonte N, Cova P, Kortabarria I. Comparison of the heat transfer capabilities of conventional single- and two-phase cooling systems for an electric vehicle IGBT power module. IEEE Trans Power Electron 2019;34(5):4185–94.
- [260] Kim J. Spray cooling heat transfer: the state of the art. Int J Heat Fluid Flow 2007;28(4):753–67.
- [261] Gould K, Cai SQ, Neft C, Bhunia A. Liquid jet impingement cooling of a silicon carbide power conversion module for vehicle applications. IEEE Trans Power Electron 2015;30(6):2975–84.
- [262] Clark MD, Weibel JA, Garimella SV. Identification of the dominant heat transfer mechanisms during confined two-phase jet impingement. IEEE intersociety conference on thermal and thermomechanical phenomena in electronic systems (ITherm). 2018. p. 424–8.
- [263] Bostanci H, Ee DV, Saarloos BA, Rini DP, Chow LC. Thermal management of power inverter modules at high fluxes via two-phase spray cooling. IEEE Trans Compon Packag Manuf Technol 2012;2(9):1480–5.
- [264] Bharathan D, Hassani V. Spray cooling: an assessment for use with automotive power electronics applications, Tech. rep. National Renewable Energy Laboratory; 2005.
- [265] Turek LJ, Rini DP, Saarloos BA, Chow LC. Evaporative spray cooling of power electronics using high temperature coolant. Conference on thermal and thermomechanical phenomena in electronic systems. 2008. p. 346–51.
- [266] Mertens R, C.L., Sundaram Ke a. Spray cooling of igt devices. J Electron Packag 2007;129(3):316–23.
- [267] Parida PR, Ekkad SV, Ngo K. Impingement-based high performance cooling configurations for automotive power converters. Int J Heat Mass Transf 2012;55(4):834–47.
- [268] Mouawad B, Skuriat R, Li J, Johnson CM, DiMarino C. Development of a highly integrated 10 kv sic mosfet power module with a direct jet impingement cooling system. International symposium on power semiconductor devices and ICs (ISPSD). 2018. p. 256–9.
- [269] Zhou F, Jung KW, Fukuoka Y, Dede EM. Chip-scale cooling of power semiconductor devices: fabrication of jet impingement design. International symposium on power semiconductor devices and ICs (ISPSD). 2018. p. 516–9.
- [270] Bhunia A, Chen C-L. Jet impingement cooling of an inverter module in the harsh environment of a hybrid vehicle. Technical conference and exhibition on integration and packaging of MEMS, vol. 4. 2005. p. 561–7.